Accepted Manuscript

An integrated theoretical-experimental approach to understand facilitated proton transfer-electron transfer coupled reactions at thick-film modified electrodes

Franco Martín Zanotto, Tamara Ayelén Hernández, Ricardo Ariel Fernández, Sergio Alberto Dassie

PII: S0013-4686(18)31545-7

DOI: 10.1016/j.electacta.2018.07.053

Reference: EA 32250

To appear in: *Electrochimica Acta*

Received Date: 28 May 2018

Revised Date: 26 June 2018

Accepted Date: 10 July 2018

Please cite this article as: Franco.Martí. Zanotto, Tamara.Ayelé. Hernández, R.A. Fernández, S.A. Dassie, An integrated theoretical-experimental approach to understand facilitated proton transfer-electron transfer coupled reactions at thick-film modified electrodes, *Electrochimica Acta* (2018), doi: 10.1016/j.electacta.2018.07.053.

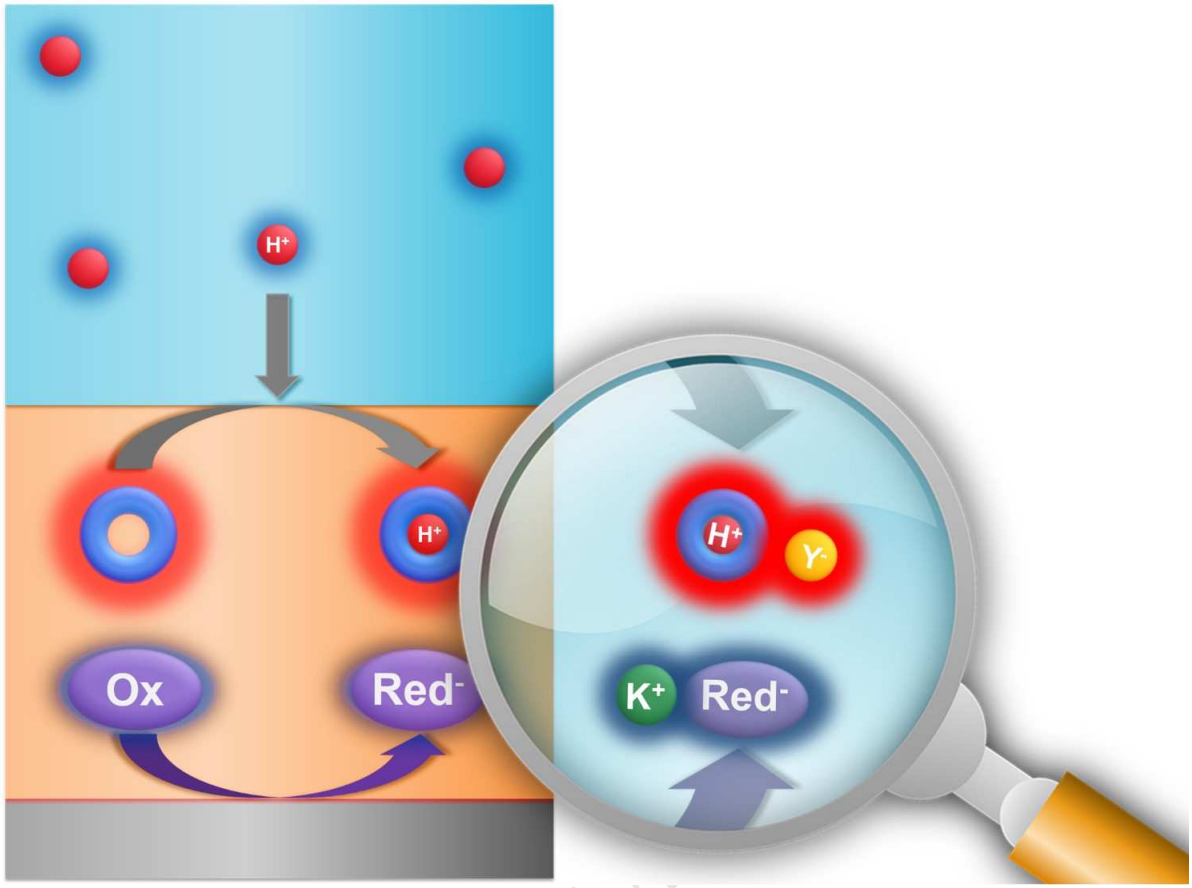

An integrated theoretical-experimental approach to understand facilitated proton transfer-electron transfer coupled reactions at thick-film modified electrodes.

Franco Martín Zanotto[1,2], Tamara Ayelén Hernández[1,2], Ricardo Ariel Fernández[1,2,*], Sergio Alberto Dassie[1,2]

[1] Departamento de Fisicoquímica. Facultad de Ciencias Químicas. Universidad Nacional de Córdoba. Ciudad Universitaria. X5000HUA. Córdoba. Argentina.

[2] Instituto de Investigaciones en Fisicoquímica de Córdoba (INFIQC), CONICET. Ciudad Universitaria. X5000HUA. Córdoba. Argentina.

Abstract

The main purpose of the current work is to generalize the analytical model for the facilitated proton transfer-electron transfer coupled reactions at thick organic film-modified electrodes, including ion pairing in the organic phase and considering non-ideal electrolyte solutions in both phases. The main equations to calculate half-wave potentials developed in this model allow the simulation of different chemical systems, comprising hydrophilic and hydrophobic neutral weak bases, at different experimental conditions such as pH, organic phase to aqueous phase volume ratio, and concentration ratios between the redox probe and the transferring protonated species. The model was checked against experimental voltammetric responses measured with the transfer of Tylosin A at the water|1,2-dichloroethene interface. Consequently, we present here an integrated theoretical-

experimental approach in order to compare the results of our previous model [Zanotto et al. Electrochim. Acta 258 (2017) 727–734] with experimental data from Tylosin A and predicted half-wave potentials.

Keywords: ion transfer-electron transfer coupled reactions; thick-film modified electrodes; protonatable species transfer; ion pairing; non-ideal electrolyte solutions.

*Corresponding author: Te/Fax: ++54-351-4334188.

e-mail address: afernandez@fcq.unc.edu.ar

1. Introduction

In recent years, the transfer of weak acids and bases across liquid|liquid interfaces has attracted the attention of many research groups [1–37]. The complementary synergy between experimental and theoretical approaches has allowed to understand the strong dependence of either protonated species or proton facilitated transfers on the pH of the aqueous phase, volume ratio ($r = V_o V_w^{-1}$) and their partition coefficient. These processes have been widely studied in both buffered and unbuffered aqueous solutions. In particular, our research group has been focused on understanding the physicochemical processes that control the proton facilitated transfer *via* water autoprotolysis [17,21,27–29]. In the case of buffered aqueous solutions, we have examined the variation of the peak current values vs. pH or volume ratio to determine partition coefficients of neutral weak bases at the oil|water interface. These studies were based on the voltammetric responses measured in quiescent solutions [18,20] and under forced hydrodynamic conditions [31]. Additionally, we have developed models for

facilitated proton transfer or charged species transfer across liquid|liquid interfaces including ion pairing (IP) and non-ideal electrolyte solutions (NIES) to calculate the half-wave potential for neutral weak bases and acids [25,26].

Recently, we have reported a general model of a thick organic film-modified electrode to analyse facilitated proton transfer-electron transfer coupled reactions (FPT-ET reactions) in different experimental conditions, such as pH and concentration ratios between the redox probe and the transferring protonated species [38]. These results show that the main difference in behaviour of the thick organic film-modified electrode is due to the transferring species which are protonatable weak bases or permanent charged ions [39]. The presence of a weak base makes it possible to pre-concentrate (or dilute) it, and to adjust the relative amounts of charged and neutral species by handling pH and volume ratio. The possibility of tuning mid-peak potentials with the volume ratio offers a practical strategy to shift the mid-peak potential vs pH profile. Moreover, partition coefficients of neutral weak bases (e.g. drugs) can be calculated, which would not be accessible with the conventional ITIES setup [38].

The main purpose of the current work is to generalize the analytical model for the FPT-ET reactions at thick organic film-modified electrodes, including IP in the organic phase and considering NIES in both phases. The main equations to calculate half-wave potentials developed in this model allow the simulation of different chemical systems, comprising hydrophilic and hydrophobic neutral weak bases, at different experimental conditions, such as pH, volume ratio, and concentration ratios between the redox probe and the transferring protonated species. The model was checked against experimental voltammetric responses measured with the transfer of Tylosin A at the water|1,2-

dichloroethene interface. Consequently, here we present an integrated theoretical-experimental approach in order to compare the results of our previous model [38] with the Tylosin A experimental data and the predicted half-wave potentials.

2. Theory

This section presents the development of the main equations that describe the half-wave potential for the electron transfer process coupled with facilitated proton transfer or protonated species transfer. In order to deduce the model for FPT-ET reactions, the same set of assumptions as those in a previous paper were made [38], with the exception of those concerning IP and NIES (assumptions (9) and (10) in Ref. [38]), since these effects are explicitly taken into account. The principal symbols used in this work are summarized in Table 1.

The solid|liquid (S|L) interface is defined to be at $x = 0$ and the liquid|liquid (L|L) interface at $x = L$ (as shown in Fig. 1).

2.1 Activity coefficients

In the analysed system, different types of species in solution were considered: neutral undissociated species, fully solvated or free ions and ion pairs of overall zero charge. For charged species, Fraenkel's smaller-ion shell (SiS) model was used, [40–44] which consists in a generalization of the classical Debye-Hückel (DH) theory, in order to take into account the different sizes of spherically symmetric charged species to calculate their activity coefficients. The activity coefficients for the different cationic and anionic species in each phase α are given respectively by:

$$\log\left(\gamma_{+}^{\alpha}\right)=-z_{+}^{2}\frac{A_{\alpha}}{B_{\alpha}}\left(\frac{\kappa_{\alpha}}{1+\kappa_{\alpha}a_{\alpha}}\right)\left\{1-\frac{2\exp\left[\kappa_{\alpha}\left(a_{\alpha}-b_{+,\alpha}\right)\right]-\kappa_{\alpha}\left(a_{\alpha}-b_{+,\alpha}\right)-2}{1+\kappa_{\alpha}b_{+,\alpha}}\right\} \quad (1)$$

$$\log\left(\gamma_{-}^{\alpha}\right)=-z_{-}^{2}\frac{A_{\alpha}}{B_{\alpha}}\left(\frac{\kappa_{\alpha}}{1+\kappa_{\alpha}a_{\alpha}}\right)\left\{1-\frac{2\exp\left[\kappa_{\alpha}\left(b_{-,\alpha}-a_{\alpha}\right)\right]-\kappa_{\alpha}\left(b_{-,\alpha}-a_{\alpha}\right)-2}{1+\kappa_{\alpha}b_{-,\alpha}}\right\} \quad (2)$$

where: $A_{\alpha}=\left(\frac{\delta_{\alpha}}{2\ln 10}\right)B_{\alpha}$ with: $\delta_{\alpha}=\frac{q_e^2}{4\pi\varepsilon_0\varepsilon_{\alpha}k_{\mathrm{B}}T}$, and $B_{\alpha}=\left[\frac{8\pi\delta_{\alpha}\sigma_{\alpha}N_{\mathrm{A}}}{10^3}\right]^{\frac{1}{2}}$

$\kappa_{\alpha}=\left[\frac{8\pi\delta_{\alpha}\sigma_{\alpha}N_{\mathrm{A}}}{10^3}\times I_{\alpha}\right]^{\frac{1}{2}}$ with: $I_{\alpha}=\frac{1}{2}\sum_i m_i z_i^2$ being the ionic strength; also, $b_{+,\alpha}$; $b_{-,\alpha}$ and a_{α} represent the closest internuclear cation-cation, anion-anion and anion-cation distances, respectively. Without loss of generality, we consider that all ions have the same size,

In the particular case of ion pairs of overall zero charge, activity coefficients are given by a different expression which describes the association of oppositely charged ions in electrolyte solutions [45–48]:

$$\ln\left(\gamma_{\text{ion pair}}^{\text{o}}\right)=\left[\frac{V^{\text{intr}}\left(V^{\text{intr}}-V^{0}\right)}{10^3\,\kappa_{\mathrm{T}}RT}\right]I_{\mathrm{o}} \quad (3)$$

where V^{intr} is the sum of the intrinsic volumes of the cation and anion, V^0 is the standard partial molar volume of the electrolyte [45,46,48–54]; I_{o} is the ionic strength of the

electrolyte in the organic phase and κ_T is the isothermal compressibility of the non-aqueous solvent [55,56].

2.2 Corrections for non-ideality of equilibrium constants

Fig. 1 shows diagrams of the chemical and electrochemical equilibria taking place in the system. The species present in solution are considered at equilibrium. Supporting electrolyte is explicitly considered in both phases: KY represents the organic electrolyte and MX the aqueous one. A redox couple is present in the organic phase, initially as an oxidized species (Ox). The acid-base equilibrium of a weak base initially dissolved in the aqueous phase as HBX is incorporated, represented in each phase α by:

$$HB^+(\alpha) \rightleftharpoons H^+(\alpha) + B(\alpha) \quad \text{(R1)}$$

Ion pair equilibria in the organic phase are the following:

$$K^+(o) + Y^-(o) \rightleftharpoons KY(o) \quad \text{(R2)}$$

$$K^+(o) + Red^-(o) \rightleftharpoons KRed(o) \quad \text{(R3)}$$

$$HB^+(o) + Y^-(o) \rightleftharpoons HBY(o) \quad \text{(R4)}$$

In addition, heterogeneous equilibria in the system are represented by:

$$Ox(o) + e^- \rightleftharpoons Red^-(o) \quad \text{(R5)}$$

$$B(w) \rightleftharpoons B(o) \quad \text{(R6)}$$

$H^+(w) \rightleftharpoons H^+(o)$ (R7)

$HB^+(w) \rightleftharpoons HB^+(o)$ (R8)

$H^+(w) + B(o) \rightleftharpoons HB^+(o)$ (R9)

According to these equilibria, the apparent acid dissociation constant for species HB^+ in phase α is defined as follows:

$$K'^{\alpha}_{a,HB^+} = K^{\alpha}_{a,HB^+} \frac{\gamma^{\alpha}_{HB^+}}{\gamma^{\alpha}_{H^+}\gamma^{\alpha}_{B}} = \frac{c^{\alpha}_{H^+} c^{\alpha}_{B}}{c^{\alpha}_{HB^+}} \quad (4)$$

where K^{α}_{a,HB^+} is the acid dissociation constant in the α phase corresponding to reaction (R1). While relevant effective ion pair formation constants, which involve the organic supporting electrolyte ions, Red^- and HB^+ species, are defined as:

$$K'_{SE} = K_{SE} \frac{\gamma^{O}_{K^+}\gamma^{O}_{Y^-}}{\gamma^{O}_{KY}} = \frac{c^{O}_{KY}}{c^{O}_{K^+} c^{O}_{Y^-}} \quad (5)$$

$$K'_{KRed} = K_{KRed} \frac{\gamma^{O}_{K^+}\gamma^{O}_{Red^-}}{\gamma^{O}_{KRed}} = \frac{c^{O}_{KRed}}{c^{O}_{K^+} c^{O}_{Red^-}} \quad (6)$$

$$K'_{HBY} = K_{HBY} \frac{\gamma^{O}_{HB^+}\gamma^{O}_{Y^-}}{\gamma^{O}_{HBY}} = \frac{c^{O}_{HBY}}{c^{O}_{HB^+} c^{O}_{Y^-}} \quad (7)$$

where K_{SE}, K_{KRed} and K_{HBY} are the ion-pair equilibrium constants corresponding to reactions (R2) to (R4), respectively. For the determination of the effective partition coefficient of the neutral species, activity coefficients are assumed to be equal in both phases and close to unity [26,57], according to (R5):

$$K'_{\mathrm{D,B}} = K_{\mathrm{D,B}} = \frac{c_{\mathrm{B}}^{\mathrm{O}}}{c_{\mathrm{B}}^{\mathrm{W}}} \tag{8}$$

2.3 Half-wave potential as a function of pH

Given that the external applied potential is distributed between the S|L interface and the L|L interface [39,58,59], in this section, equations are developed to describe the value of the external applied potential when the interface that involves the limiting charge transfer reaction is at its half-wave potential. Here, the half wave potential corresponding to the facilitated proton transfer process is $\Delta_{\mathrm{O}}^{\mathrm{W}}\phi_{1/2}$, while $\Delta_{\mathrm{O}}^{\mathrm{S}}\phi_{1/2}$ corresponds to the electron transfer process.

Considering the flux balance of Ox and Red^- species, the following expression can be deduced [25,60,61] (for the deduction of this expression see the first section of the Supplementary Material):

$$\sqrt{D_{\mathrm{Ox}}^{\mathrm{O}}}\, c_{\mathrm{Ox}}^{\mathrm{init}} = \sqrt{D_{\mathrm{Ox}}^{\mathrm{O}}}\, c_{\mathrm{Ox}}^{\mathrm{O}}(0,t) + \sqrt{\bar{D}}\left[\, c_{\mathrm{Red}^-}^{\mathrm{O}}(0,t) + c_{\mathrm{KRed}}^{\mathrm{O}}(0,t) \,\right] \tag{9}$$

where $\bar{D}\left(= \dfrac{D_{\mathrm{Red}^-}^{\mathrm{O}} + D_{\mathrm{KRed}}^{\mathrm{O}}\alpha_{\mathrm{SE}}c_{\mathrm{SE}}^{\mathrm{O}}K'_{\mathrm{KRed}}}{1+\alpha_{\mathrm{SE}}c_{\mathrm{SE}}^{\mathrm{O}}K'_{\mathrm{KRed}}}\right)$ is the effective diffusion coefficient [8], being $c_{\mathrm{SE}}^{\mathrm{O}}$ the bulk concentration of the organic supporting electrolyte and $\alpha_{\mathrm{SE}}\left(= c_{\mathrm{K}^+}^{\mathrm{O}} / c_{\mathrm{SE}}^{\mathrm{O}}\right)$ the degree of its dissociation in the organic phase [26,62,63]. The fraction of free ion can be calculated from $K'_{\mathrm{SE}} = \dfrac{1-\alpha_{\mathrm{SE}}}{\alpha_{\mathrm{SE}}^2 c_{\mathrm{SE}}^{\mathrm{O}}}$. This approximation is valid when the bulk concentration of the counter ion of the supporting electrolyte is much higher than that of the redox species [25]. Here,

$D^{O}_{Red^-}$ and D^{O}_{KRed} are diffusion coefficients of Red^- and KRed in the organic phase, respectively.

Since the electron transfer and ion transfer processes must produce the same net current values, and both interfaces present the same surface area, the same amount of product at each interface must be generated, thus, the following expression can be written:

$$\sqrt{D^{O}}\left[c^{O}_{HB^+}(L,t)+c^{O}_{HBY}(L,t)\right]=\sqrt{\overline{D}}\left[c^{O}_{Red^-}(0,t)+c^{O}_{KRed}(0,t)\right] \quad (10)$$

where D^{α} is the diffusion coefficient of HB^+, HBY, and B in phase α, assumed to be common for all species in each phase.

When the redox probe concentration is in defect with respect to the total concentration of the weak base, the electron transfer process limits the current for the ion transfer process. In particular, it possible to write:

$$\sqrt{D^{O}_{Ox}}c^{O}_{Ox}(0,\Delta^{S}_{O}\phi_{1/2})=\sqrt{\overline{D}}\left[c^{O}_{Red^-}(0,\Delta^{S}_{O}\phi_{1/2})+c^{O}_{KRed}(0,\Delta^{S}_{O}\phi_{1/2})\right] \quad (11)$$

where, $c_i^{\alpha}(x,\Delta^{S}_{O}\phi_{1/2})$, represents the concentration of the *i* species in phase α at x position at the time when the Galvani potential difference at the S|L interface is equal to its half-wave potential, $\Delta^{S}_{O}\phi_{1/2}$.

In this particular situation, the previous equation also implies:

$$\frac{1}{2}\sqrt{D^{O}_{Ox}}c^{init}_{Ox}=\sqrt{D^{O}_{Ox}}c^{O}_{Ox}(0,\Delta^{S}_{O}\phi_{1/2}) \quad (12)$$

$$\frac{1}{2}\sqrt{D^{O}_{Ox}}c^{init}_{Ox}=\sqrt{\overline{D}}\left[c^{O}_{Red^-}(0,\Delta^{S}_{O}\phi_{1/2})+c^{O}_{KRed}(0,\Delta^{S}_{O}\phi_{1/2})\right] \quad (13)$$

Additionally, since the ion transfer and electron transfer reactions are coupled, total product for each of them must be equal, and thus linked by:

$$\sqrt{\overline{D}}\left[c^{\mathrm{O}}_{\mathrm{Red}^-}(0,\Delta^{\mathrm{S}}_{\mathrm{O}}\phi_{1/2})+c^{\mathrm{O}}_{\mathrm{KRed}}(0,\Delta^{\mathrm{S}}_{\mathrm{O}}\phi_{1/2})\right]=\sqrt{D^{\mathrm{O}}}\left[c^{\mathrm{O}}_{\mathrm{HB}^+}(L,\Delta^{\mathrm{S}}_{\mathrm{O}}\phi_{1/2})+c^{\mathrm{O}}_{\mathrm{HBY}}(L,\Delta^{\mathrm{S}}_{\mathrm{O}}\phi_{1/2})\right] \quad (14)$$

According to previous works [25,61], the total interfacial concentration of weak base species can be expressed as follows:

$$\sqrt{D^{\mathrm{W}}}c^{\mathrm{init}}_{\mathrm{B,tot}}=\sqrt{D^{\mathrm{O}}}\left[c^{\mathrm{O}}_{\mathrm{HB}^+}(L,\Delta^{\mathrm{S}}_{\mathrm{O}}\phi_{1/2})+c^{\mathrm{O}}_{\mathrm{HBY}}(L,\Delta^{\mathrm{S}}_{\mathrm{O}}\phi_{1/2})+c^{\mathrm{O}}_{\mathrm{B}}(L,\Delta^{\mathrm{S}}_{\mathrm{O}}\phi_{1/2})\right]+\sqrt{D^{\mathrm{W}}}\left[c^{\mathrm{W}}_{\mathrm{HB}^+}(L,\Delta^{\mathrm{S}}_{\mathrm{O}}\phi_{1/2})+c^{\mathrm{W}}_{\mathrm{B}}(L,\Delta^{\mathrm{S}}_{\mathrm{O}}\phi_{1/2})\right]$$

(15)

Substituing Eq. (13) in Eq. (14) and subtracting the result from Eq. (15), the following expression is obtained:

$$\sqrt{D^{\mathrm{W}}}c^{\mathrm{init}}_{\mathrm{B,tot}}-\frac{1}{2}\sqrt{D^{\mathrm{O}}_{\mathrm{Ox}}}c^{\mathrm{init}}_{\mathrm{Ox}}=\sqrt{D^{\mathrm{O}}}c^{\mathrm{O}}_{\mathrm{B}}(L,\Delta^{\mathrm{S}}_{\mathrm{O}}\phi_{1/2})+\sqrt{D^{\mathrm{W}}}c^{\mathrm{W}}_{\mathrm{HB}^+}(L,\Delta^{\mathrm{S}}_{\mathrm{O}}\phi_{1/2})+\sqrt{D^{\mathrm{W}}}c^{\mathrm{W}}_{\mathrm{B}}(L,\Delta^{\mathrm{S}}_{\mathrm{O}}\phi_{1/2})$$

(16)

Taking into account acid-base and partition equilibria, Eq. (16) can be expressed in terms of $c^{\mathrm{O}}_{\mathrm{HB}^+}(L,\Delta^{\mathrm{S}}_{\mathrm{O}}\phi_{1/2})$ and $c^{\mathrm{O}}_{\mathrm{H}^+}(L,\Delta^{\mathrm{S}}_{\mathrm{O}}\phi_{1/2})$:

$$\sqrt{D^{\mathrm{W}}}c^{\mathrm{init}}_{\mathrm{B,tot}}-\frac{1}{2}\sqrt{D^{\mathrm{O}}_{\mathrm{Ox}}}c^{\mathrm{init}}_{\mathrm{Ox}}=\frac{c^{\mathrm{O}}_{\mathrm{HB}^+}(L,\Delta^{\mathrm{S}}_{\mathrm{O}}\phi_{1/2})}{c^{\mathrm{O}}_{\mathrm{H}^+}(L,\Delta^{\mathrm{S}}_{\mathrm{O}}\phi_{1/2})}K'^{\mathrm{O}}_{\mathrm{a,HB}^+}\left[\sqrt{\frac{D^{\mathrm{O}}}{D^{\mathrm{W}}}}+\frac{c^{\mathrm{W}}_{\mathrm{H}^+}(L,\Delta^{\mathrm{S}}_{\mathrm{O}}\phi_{1/2})}{K'^{\mathrm{W}}_{\mathrm{a,HB}^+}K'_{\mathrm{D,B}}}+\frac{1}{K'_{\mathrm{D,B}}}\right] \quad (17)$$

Since $c^{\mathrm{O}}_{\mathrm{H}^+}(L,\Delta^{\mathrm{S}}_{\mathrm{O}}\phi_{1/2})$ also can be expressed in terms of the L|L interface potential and $c^{\mathrm{w}}_{\mathrm{H}^+}(L,\Delta^{\mathrm{S}}_{\mathrm{O}}\phi_{1/2})$ as follows:

$$c_{\mathrm{H^+}}^{\mathrm{O}}(L,\Delta_{\mathrm{O}}^{\mathrm{S}}\phi_{1/2}) = c_{\mathrm{H^+}}^{\mathrm{W}}(L,\Delta_{\mathrm{O}}^{\mathrm{S}}\phi_{1/2})\exp\left\{\frac{F}{RT}\left[\Delta_{\mathrm{O}}^{\mathrm{W}}\phi(\Delta_{\mathrm{O}}^{\mathrm{S}}\phi_{1/2}) - \Delta_{\mathrm{O}}^{\mathrm{W}}\phi_{\mathrm{H^+}}^{\mathrm{o'}}\right]\right\} \tag{18}$$

where, $\Delta_{\mathrm{O}}^{\mathrm{W}}\phi\left(\Delta_{\mathrm{O}}^{\mathrm{S}}\phi_{1/2}\right)$ is the L|L interface potential value when the S|L interface potential is equal to $\Delta_{\mathrm{O}}^{\mathrm{S}}\phi_{1/2}$, the following expression for $c_{\mathrm{HB^+}}^{\mathrm{O}}(L,\Delta_{\mathrm{O}}^{\mathrm{S}}\phi_{1/2})$ can be obtained:

$$c_{\mathrm{HB^+}}^{\mathrm{O}}(L,\Delta_{\mathrm{O}}^{\mathrm{S}}\phi_{1/2}) = \left(c_{\mathrm{B,tot}}^{\mathrm{init}} - \frac{1}{2}\sqrt{\frac{D_{\mathrm{Ox}}^{\mathrm{O}}}{D^{\mathrm{W}}}}c_{\mathrm{Ox}}^{\mathrm{init}}\right)\exp\left\{\frac{F}{RT}\left[\Delta_{\mathrm{O}}^{\mathrm{W}}\phi\left(\Delta_{\mathrm{O}}^{\mathrm{S}}\phi_{1/2}\right) - \Delta_{\mathrm{O}}^{\mathrm{W}}\phi_{\mathrm{H^+}}^{\mathrm{o'}}\right]\right\}\frac{1}{K_{\mathrm{a,HB^+}}^{\mathrm{'O}}}\left[\frac{K_{\mathrm{a,HB^+}}^{\mathrm{'W}}K_{\mathrm{D,B}}^{'}c_{\mathrm{H^+}}^{\mathrm{W}}(L,\Delta_{\mathrm{O}}^{\mathrm{S}}\phi_{1/2})}{K_{\mathrm{a,HB^+}}^{\mathrm{'W}}K_{\mathrm{D,B}}^{'}\sqrt{\frac{D^{\mathrm{O}}}{D^{\mathrm{W}}}} + c_{\mathrm{H^+}}^{\mathrm{W}}(L,\Delta_{\mathrm{O}}^{\mathrm{S}}\phi_{1/2}) + K_{\mathrm{a,HB^+}}^{\mathrm{'W}}}\right] \tag{19}$$

In addition, if the formal standard reduction potential is defined in terms of the standard reduction potential and activity coefficients as follows:

$$\Delta_{\mathrm{O}}^{\mathrm{S}}\phi^{\mathrm{o'}} = \Delta_{\mathrm{O}}^{\mathrm{S}}\phi^{\mathrm{o}} + \frac{RT}{F}\ln\left(\frac{\gamma_{\mathrm{Ox}}^{\mathrm{O}}}{\gamma_{\mathrm{Red^-}}^{\mathrm{O}}}\right) \tag{20}$$

the Nernst equation for the S|L interface at the half-wave potential can be stated as:

$$\Delta_{\mathrm{O}}^{\mathrm{S}}\phi_{1/2} = \Delta_{\mathrm{O}}^{\mathrm{S}}\phi^{\mathrm{o'}} + \frac{RT}{F}\ln\left(\frac{c_{\mathrm{Ox}}^{\mathrm{O}}(0,\Delta_{\mathrm{O}}^{\mathrm{S}}\phi_{1/2})}{c_{\mathrm{Red^-}}^{\mathrm{O}}(0,\Delta_{\mathrm{O}}^{\mathrm{S}}\phi_{1/2})}\right) \tag{21}$$

which can be expressed as:

$$\Delta_{\mathrm{O}}^{\mathrm{S}}\phi_{1/2} = \Delta_{\mathrm{O}}^{\mathrm{S}}\phi^{\mathrm{o'}} + \frac{RT}{F}\ln\left[2\left(\frac{\sqrt{D^{\mathrm{O}}\overline{D}}}{D_{\mathrm{Ox}}^{\mathrm{O}}}\right)\frac{\left(1+K_{\mathrm{HBY}}^{'}\alpha_{\mathrm{SE}}c_{\mathrm{SE}}^{\mathrm{O}}\right)\left(1+K_{\mathrm{KRed}}^{'}\alpha_{\mathrm{SE}}c_{\mathrm{SE}}^{\mathrm{O}}\right)c_{\mathrm{HB^+}}^{\mathrm{O}}(L,\Delta_{\mathrm{O}}^{\mathrm{S}}\phi_{1/2})}{c_{\mathrm{Ox}}^{\mathrm{init}}}\right] \tag{22}$$

Working with Eqs. (19) and (22), and rearranging:

$$\Delta_{\mathrm{O}}^{\mathrm{S}}\phi_{1/2}-\Delta_{\mathrm{O}}^{\mathrm{W}}\phi\left(\Delta_{\mathrm{O}}^{\mathrm{S}}\phi_{1/2}\right)=\Delta_{\mathrm{O}}^{\mathrm{S}}\phi^{\mathrm{o}'}-\Delta_{\mathrm{O}}^{\mathrm{W}}\phi_{\mathrm{H}^+}^{\mathrm{o}'}+\frac{RT}{F}\ln\left(\frac{K_{\mathrm{a,HB}^+}^{\mathrm{W}}K_{\mathrm{D,B}}^{'}}{K_{\mathrm{a,HB}^+}^{'\mathrm{O}}}\right)$$
$$+\frac{RT}{F}\ln\left\{2\left(\frac{\sqrt{D^{\mathrm{O}}\bar{D}}}{D_{\mathrm{Ox}}^{\mathrm{O}}}\right)\frac{\left(c_{\mathrm{B,tot}}^{\mathrm{init}}-\frac{1}{2}\sqrt{\frac{D_{\mathrm{Ox}}^{\mathrm{O}}}{D^{W}}}c_{\mathrm{Ox}}^{\mathrm{init}}\right)\left(1+K_{\mathrm{HBY}}^{'}\alpha_{\mathrm{SE}}c_{\mathrm{SE}}^{\mathrm{O}}\right)\left(1+K_{\mathrm{KRed}}^{'}\alpha_{\mathrm{SE}}c_{\mathrm{SE}}^{\mathrm{O}}\right)}{c_{\mathrm{Ox}}^{\mathrm{init}}}\right\} \quad (23)$$
$$+\frac{RT}{F}\ln\left[\frac{c_{\mathrm{H}^+}^{\mathrm{W}}(L,\Delta_{\mathrm{O}}^{\mathrm{S}}\phi_{1/2})}{K_{\mathrm{a,HB}^+}^{\mathrm{W}}K_{\mathrm{D,B}}^{'}\sqrt{\frac{D^{\mathrm{O}}}{D^{\mathrm{W}}}}+c_{\mathrm{H}^+}^{\mathrm{W}}(L,\Delta_{\mathrm{O}}^{\mathrm{S}}\phi_{1/2})+K_{\mathrm{a,HB}^+}^{\mathrm{W}}}\right]$$

In this expression, the term: $\Delta_{\mathrm{O}}^{\mathrm{S}}\phi_{1/2}-\Delta_{\mathrm{O}}^{\mathrm{W}}\phi\left(\Delta_{\mathrm{O}}^{\mathrm{S}}\phi_{1/2}\right)$ is the external applied potential when the S|L interface Galvani potential difference is $\Delta_{\mathrm{O}}^{\mathrm{S}}\phi_{1/2}$. Writing $\Delta_{\mathrm{O}}^{\mathrm{W}}\phi_{\mathrm{H}^+}^{\mathrm{o}'}$ as a function of $\Delta_{\mathrm{O}}^{\mathrm{W}}\phi_{\mathrm{HB}^+}^{\mathrm{o}'}$ and apparent equilibrium constants, a simpler expression for $\Delta_{\mathrm{O}}^{\mathrm{S}}\phi_{1/2}-\Delta_{\mathrm{O}}^{\mathrm{W}}\phi\left(\Delta_{\mathrm{O}}^{\mathrm{S}}\phi_{1/2}\right)$ is obtained:

$$\Delta_{\mathrm{O}}^{\mathrm{S}}\phi_{1/2}-\Delta_{\mathrm{O}}^{\mathrm{W}}\phi\left(\Delta_{\mathrm{O}}^{\mathrm{S}}\phi_{1/2}\right)=\Delta_{\mathrm{O}}^{\mathrm{S}}\phi^{\mathrm{o}'}-\Delta_{\mathrm{O}}^{\mathrm{W}}\phi_{\mathrm{HB}^+}^{\mathrm{o}'}+\frac{RT}{F}\ln\left\{2\left(\frac{\sqrt{D^{\mathrm{O}}\bar{D}}}{D_{\mathrm{Ox}}^{\mathrm{O}}}\right)\frac{\left(c_{\mathrm{B,tot}}^{\mathrm{init}}-\frac{1}{2}\sqrt{\frac{D_{\mathrm{Ox}}^{\mathrm{O}}}{D^{W}}}c_{\mathrm{Ox}}^{\mathrm{init}}\right)\left(1+K_{\mathrm{HBY}}^{'}\alpha_{\mathrm{SE}}c_{\mathrm{SE}}^{\mathrm{O}}\right)\left(1+K_{\mathrm{KRed}}^{'}\alpha_{\mathrm{SE}}c_{\mathrm{SE}}^{\mathrm{O}}\right)}{c_{\mathrm{Ox}}^{\mathrm{init}}}\right\}$$
$$+\frac{RT}{F}\ln\left[\frac{c_{\mathrm{H}^+}^{\mathrm{W}}(L,\Delta_{\mathrm{O}}^{\mathrm{S}}\phi_{1/2})}{K_{\mathrm{a,HB}^+}^{\mathrm{W}}K_{\mathrm{D,B}}^{'}\sqrt{\frac{D^{\mathrm{O}}}{D^{\mathrm{W}}}}+c_{\mathrm{H}^+}^{\mathrm{W}}(L,\Delta_{\mathrm{O}}^{\mathrm{S}}\phi_{1/2})+K_{\mathrm{a,HB}^+}^{\mathrm{W}}}\right]$$

(24)

As mentioned in our previous work [38], it is important to note the difference between the analytical concentration of B, $c_{\mathrm{B}}^{\mathrm{a}}$, which corresponds to the amount of HBX dissolved in the aqueous phase, and the total initial concentration of B, $c_{\mathrm{B,tot}}^{\mathrm{init}}$, which is a result of the partition and acid-base equilibria of the weak base in the biphasic system, and is highly dependent on the volume ratio [18]. The initial concentration of the base B in the

organic phase ($c_{\mathrm{B}}^{\mathrm{O}}$) and the total concentration of weak base, protonated or not, in the aqueous phase ($c_{\mathrm{B,tot}}^{\mathrm{W}}$) can be expressed as a function of $c_{\mathrm{B}}^{\mathrm{a}}$ by the following reasoning:

$$c_{\mathrm{B}}^{\mathrm{O}}(x,0)=\left(\frac{\alpha_{\mathrm{B}}K_{\mathrm{D,B}}^{'}}{1+r\alpha_{\mathrm{B}}K_{\mathrm{D,B}}^{'}}\right)c_{\mathrm{B}}^{\mathrm{a}} \tag{25}$$

$$c_{\mathrm{B,tot}}^{\mathrm{W}}(x,0)=\left(\frac{1}{1+r\alpha_{\mathrm{B}}K_{\mathrm{D,B}}^{'}}\right)c_{\mathrm{B}}^{\mathrm{a}} \tag{26}$$

where $\alpha_{\mathrm{B}}=\dfrac{K_{\mathrm{a,HB^{+}}}^{'\mathrm{W}}}{c_{\mathrm{H^{+}}}^{\mathrm{w}}+K_{\mathrm{a,HB^{+}}}^{'\mathrm{W}}}$.

Particularly, at t = 0 [3,4,25,28,29]:

$$c_{\mathrm{B,tot}}^{\mathrm{init}}=\sqrt{\frac{D^{\mathrm{O}}}{D^{\mathrm{W}}}}c_{\mathrm{B}}^{\mathrm{O}}(x,0)+c_{\mathrm{B}}^{\mathrm{W}}(x,0) \tag{27}$$

and this implies:

$$c_{\mathrm{B,tot}}^{\mathrm{init}}=\left(\frac{1+\sqrt{\frac{D^{\mathrm{O}}}{D^{\mathrm{W}}}}\alpha_{\mathrm{B}}K_{\mathrm{D,B}}^{'}}{1+r\alpha_{\mathrm{B}}K_{\mathrm{D,B}}^{'}}\right)c_{\mathrm{B}}^{\mathrm{a}} \tag{28}$$

Finally, by replacing Eq. (28) in Eq. (24), the main general expression for $\Delta_{\mathrm{O}}^{\mathrm{S}}\phi_{1/2}-\Delta_{\mathrm{O}}^{\mathrm{W}}\phi\left(\Delta_{\mathrm{O}}^{\mathrm{S}}\phi_{1/2}\right)$ is obtained:

$$\Delta_{\mathrm{O}}^{\mathrm{S}}\phi_{1/2}-\Delta_{\mathrm{O}}^{\mathrm{W}}\phi\left(\Delta_{\mathrm{O}}^{\mathrm{S}}\phi_{1/2}\right)=\Delta_{\mathrm{O}}^{\mathrm{S}}\phi^{\mathrm{o}'}-\Delta_{\mathrm{O}}^{\mathrm{W}}\phi_{\mathrm{HB}^+}^{\mathrm{o}'}$$
$$+\frac{RT}{F}\ln\left\{2\left(\frac{\sqrt{D^{\mathrm{O}}\bar{D}}}{D_{\mathrm{Ox}}^{\mathrm{O}}}\right)\frac{\left[c_{\mathrm{B}}^{\mathrm{a}}\left(\frac{1+\sqrt{\frac{D^{\mathrm{O}}}{D^{\mathrm{W}}}}\alpha_{\mathrm{B}}K_{\mathrm{D,B}}^{'}}{1+r\alpha_{\mathrm{B}}K_{\mathrm{D,B}}^{'}}\right)-\frac{1}{2}\sqrt{\frac{D_{\mathrm{Ox}}^{\mathrm{O}}}{D^{\mathrm{W}}}}c_{\mathrm{Ox}}^{\mathrm{init}}\right]\left(1+K_{\mathrm{HBY}}^{'}\alpha_{\mathrm{SE}}c_{\mathrm{SE}}^{\mathrm{O}}\right)\left(1+K_{\mathrm{KRed}}^{'}\alpha_{\mathrm{SE}}c_{\mathrm{SE}}^{\mathrm{O}}\right)}{c_{\mathrm{Ox}}^{\mathrm{init}}}\right\}$$
$$+\frac{RT}{F}\ln\left[\frac{c_{\mathrm{H}^+}^{\mathrm{W}}(L,\Delta_O^S\phi_{1/2})}{K_{\mathrm{a,HB}^+}^{'\mathrm{W}}K_{\mathrm{D,B}}^{'}\sqrt{\frac{D^{\mathrm{O}}}{D^{\mathrm{W}}}}+c_{\mathrm{H}^+}^{\mathrm{W}}(L,\Delta_{\mathrm{O}}^{\mathrm{S}}\phi_{1/2})+K_{\mathrm{a,HB}^+}^{'\mathrm{W}}}\right] \quad (29)$$

This general equation can be simplified using Eq. (28) under the assumption that $c_{\mathrm{B,tot}}^{\mathrm{init}} \gg \frac{1}{2}\sqrt{D_{\mathrm{Ox}}^{\mathrm{O}}/D^{\mathrm{W}}}c_{\mathrm{Ox}}^{\mathrm{init}}$, which holds for many typical experimental setups [59], as follows:

$$\Delta_{\mathrm{O}}^{\mathrm{S}}\phi_{1/2}-\Delta_{\mathrm{O}}^{\mathrm{W}}\phi\left(\Delta_{\mathrm{O}}^{\mathrm{S}}\phi_{1/2}\right)=\Delta_{\mathrm{O}}^{\mathrm{S}}\phi^{\mathrm{o}'}-\Delta_{\mathrm{O}}^{\mathrm{W}}\phi_{\mathrm{HB}^+}^{\mathrm{o}'}+\frac{RT}{F}\ln\left[2\left(\frac{\sqrt{D^{\mathrm{O}}\bar{D}}}{D_{\mathrm{Ox}}^{\mathrm{O}}}\right)\left(1+K_{\mathrm{KRed}}^{'}\alpha_{\mathrm{SE}}c_{\mathrm{SE}}^{\mathrm{O}}\right)\left(1+K_{\mathrm{HBY}}^{'}\alpha_{\mathrm{SE}}c_{\mathrm{SE}}^{\mathrm{O}}\right)\right] \quad (30)$$
$$+\frac{RT}{F}\ln\left(\frac{c_{\mathrm{B}}^{\mathrm{a}}}{c_{\mathrm{Ox}}^{\mathrm{init}}}\right)+\frac{RT}{F}\ln\left(\frac{c_{\mathrm{H}^+}^{\mathrm{W}}(L,\Delta_O^S\phi_{1/2})}{K_{\mathrm{a,HB}^+}^{'\mathrm{W}}K_{\mathrm{D,B}}^{'}r+c_{\mathrm{H}^+}^{\mathrm{W}}(L,\Delta_O^S\phi_{1/2})+K_{\mathrm{a,HB}^+}^{'\mathrm{W}}}\right)$$

In the case that Ox species is in excess respect to the weak base, similar expressions can be found by fixing the Galvani potential difference at the L|L interface equal to its half-wave potential, $\Delta_{\mathrm{O}}^{\mathrm{W}}\phi_{1/2}$, since ion transfer is the limiting process. This allows the following expression to be written instead of Eqs. (12) to (14):

$$\frac{1}{2}\sqrt{D^{\mathrm{W}}}c_{\mathrm{B,tot}}^{\mathrm{init}}=\sqrt{D^{\mathrm{W}}}c_{\mathrm{HB}^+}^{\mathrm{W}}(0,\Delta_{\mathrm{O}}^{\mathrm{W}}\phi_{1/2})+\sqrt{D^{\mathrm{W}}}c_{\mathrm{B}}^{\mathrm{W}}(0,\Delta_{\mathrm{O}}^{\mathrm{W}}\phi_{1/2})+\sqrt{D^{\mathrm{O}}}c_{\mathrm{B}}^{\mathrm{O}}(0,\Delta_{\mathrm{O}}^{\mathrm{W}}\phi_{1/2}) \quad (31)$$

$$\frac{1}{2}\sqrt{D^{\mathrm{W}}}c_{\mathrm{B,tot}}^{\mathrm{init}}=\sqrt{D^{\mathrm{O}}}c_{\mathrm{HB}^+}^{\mathrm{O}}(L,\Delta_{\mathrm{O}}^{\mathrm{W}}\phi_{1/2})+\sqrt{D^{\mathrm{O}}}c_{\mathrm{HBY}}^{\mathrm{O}}(L,\Delta_{\mathrm{O}}^{\mathrm{W}}\phi_{1/2}) \quad (32)$$

$$\frac{1}{2}\sqrt{D^{\mathrm{W}}}c_{\mathrm{B,tot}}^{\mathrm{init}}=\sqrt{\bar{D}}\left[c_{\mathrm{Red}^-}^{\mathrm{O}}(0,\Delta_{\mathrm{O}}^{\mathrm{W}}\phi_{1/2})+c_{\mathrm{KRed}}^{\mathrm{O}}(0,\Delta_{\mathrm{O}}^{\mathrm{W}}\phi_{1/2})\right] \quad (33)$$

From these equations, by following a very similar approach as before, the main general expression for $\Delta_{\mathrm{O}}^{\mathrm{S}}\phi\left(\Delta_{\mathrm{O}}^{\mathrm{W}}\phi_{1/2}\right)-\Delta_{\mathrm{O}}^{\mathrm{W}}\phi_{1/2}$ when the weak base is in defect with respect to Ox species results:

$$\Delta_{\mathrm{O}}^{\mathrm{S}}\phi\left(\Delta_{\mathrm{O}}^{\mathrm{W}}\phi_{1/2}\right)-\Delta_{\mathrm{O}}^{\mathrm{W}}\phi_{1/2}=\Delta_{\mathrm{O}}^{\mathrm{S}}\phi^{\mathrm{o}'}-\Delta_{\mathrm{O}}^{\mathrm{W}}\phi_{\mathrm{HB}^+}^{\mathrm{o}'}+\frac{RT}{F}\ln\left[2\left(\frac{\sqrt{D^{\mathrm{O}}\bar{D}}}{D^{\mathrm{W}}}\right)\left(1+K_{\mathrm{KRed}}^{'}\alpha_{\mathrm{SE}}c_{\mathrm{SE}}^{\mathrm{O}}\right)\left(1+K_{\mathrm{HBY}}^{'}\alpha_{\mathrm{SE}}c_{\mathrm{SE}}^{\mathrm{O}}\right)\right]$$
$$+\frac{RT}{F}\ln\left[\frac{c_{\mathrm{Ox}}^{\mathrm{init}}-\frac{\sqrt{D^{\mathrm{W}}}}{\sqrt{D_{\mathrm{Ox}}}}\frac{c_{\mathrm{B}}^{\mathrm{a}}}{2}\left(\frac{1+\sqrt{\frac{D^{\mathrm{O}}}{D^{\mathrm{W}}}}\alpha_{\mathrm{B}}K_{\mathrm{D,B}}^{'}}{1+r\alpha_{\mathrm{B}}K_{\mathrm{D,B}}^{'}}\right)}{c_{\mathrm{B}}^{\mathrm{a}}}\right]$$
$$+\frac{RT}{F}\ln\left[\frac{c_{\mathrm{H}^+}^{\mathrm{W}}(L,\Delta_{\mathrm{O}}^{\mathrm{W}}\phi_{1/2})\left(K_{\mathrm{a,HB}^+}^{'\mathrm{W}}K_{\mathrm{D,B}}^{'}r+c_{\mathrm{H}^+}^{\mathrm{W}}(L,\Delta_{\mathrm{O}}^{\mathrm{W}}\phi_{1/2})+K_{\mathrm{a,HB}^+}^{'\mathrm{W}}\right)}{\left(K_{\mathrm{a,HB}^+}^{'\mathrm{W}}K_{\mathrm{D,B}}^{'}\frac{\sqrt{D^{\mathrm{O}}}}{\sqrt{D^{\mathrm{W}}}}+c_{\mathrm{H}^+}^{\mathrm{W}}(L,\Delta_{\mathrm{O}}^{\mathrm{W}}\phi_{1/2})+K_{\mathrm{a,HB}^+}^{'\mathrm{W}}\right)^2}\right] \quad (34)$$

under the assumption that $c_{\mathrm{Ox}}^{\mathrm{init}} \gg \frac{1}{2}\sqrt{D^{\mathrm{W}}/D_{\mathrm{Ox}}^{\mathrm{O}}}c_{\mathrm{B,tot}}^{\mathrm{init}}$, the following simplified expression is obtained, which is valid for certain experimental conditions [64]:

$$\Delta_{\mathrm{O}}^{\mathrm{S}}\phi\left(\Delta_{\mathrm{O}}^{\mathrm{W}}\phi_{1/2}\right)-\Delta_{\mathrm{O}}^{\mathrm{W}}\phi_{1/2}=\Delta_{\mathrm{O}}^{\mathrm{S}}\phi^{\mathrm{o}'}-\Delta_{\mathrm{O}}^{\mathrm{W}}\phi_{\mathrm{HB}^+}^{\mathrm{o}'}+\frac{RT}{F}\ln\left[2\left(\frac{\sqrt{D^{\mathrm{O}}\bar{D}}}{D^{\mathrm{W}}}\right)\left(1+K_{\mathrm{KRed}}^{'}\alpha_{\mathrm{SE}}c_{\mathrm{SE}}^{\mathrm{O}}\right)\left(1+K_{\mathrm{HBY}}^{'}\alpha_{\mathrm{SE}}c_{\mathrm{SE}}^{\mathrm{O}}\right)\right]$$
$$+\frac{RT}{F}\ln\left(\frac{c_{\mathrm{Ox}}^{\mathrm{init}}}{c_{\mathrm{B}}^{\mathrm{a}}}\right)+\frac{RT}{F}\ln\left[\frac{c_{\mathrm{H}^+}^{\mathrm{W}}(L,\Delta_{\mathrm{O}}^{\mathrm{W}}\phi_{1/2})\left(K_{\mathrm{a,HB}^+}^{\mathrm{W}}K_{D,B}^{'}r+c_{\mathrm{H}^+}^{\mathrm{W}}(L,\Delta_{\mathrm{O}}^{\mathrm{W}}\phi_{1/2})+K_{\mathrm{a,HB}^+}^{\mathrm{W}}\right)}{\left(K_{\mathrm{a,HB}^+}^{\mathrm{W}}K_{D,B}^{'}\frac{\sqrt{D^{\mathrm{O}}}}{\sqrt{D^{\mathrm{W}}}}+c_{\mathrm{H}^+}^{\mathrm{W}}(L,\Delta_{\mathrm{O}}^{\mathrm{W}}\phi_{1/2})+K_{\mathrm{a,HB}^+}^{\mathrm{W}}\right)^2}\right] \quad (35)$$

It is important to note that these equations are valid for buffered solutions, for which $c^{\mathrm{W}}_{\mathrm{H}^+}(L, \Delta^{\mathrm{W}}_{\mathrm{O}}\phi_{1/2})$ can be determined from the pH of the aqueous phase according to: $10^{-\mathrm{pH}} = \gamma^{\mathrm{W}}_{\mathrm{H}^+} c^{\mathrm{W}}_{\mathrm{H}^+}(L, \Delta^{\mathrm{W}}_{\mathrm{O}}\phi_{1/2})$.

3. Experimental methods

3.1 Chemicals

The organic supporting electrolyte was 0.038 M tetraphenylarsonium dicarbollylcobaltate (TPADCC) in 1,2-dichloroethane (1,2-DCE) (Dorwil p.a.). TPADCC was prepared as described in ref. [65]. 1,2-DCE was washed with an excess of ultrapure water in order to eliminate hydrophilic impurities. Tetracyanoquinodimethane (TCNQ) (Acros Organics, 98%) 0.23 mM in 1,2-DCE was used in all experiments, without further purification. Tylosin A tartrate (Sigma) was used without further purification and was always dissolved in the aqueous phase to a concentration of 3.0 mM. pH values were adjusted using phosphate or acetate of analytical concentration 0.5 M as buffer solutions.

3.2 Electrochemical setup

Electrochemical experiments were carried out using a commercial potentiostat-galvanostat (Autolab PGSTAT100) in the conventional three-electrode setup. A platinum sheet was used as counter-electrode. All experimental potentials are reported with respect to the reference electrode Ag|AgCl|NaCl (3.0 M). Before each experiment, the glassy carbon working electrode was mechanically polished with 0.05 mm alumina slurry on a felt cloth, rinsed with deionized water and then dried at room temperature and cycled in phosphate

buffer for 10 cycles at a sweep rate of 100 mVs^{-1}. The organic and aqueous solutions were put in contact and stirred before each experiment in order to ensure that acid-base and partition equilibria were achieved [18,20]. The organic phase and aqueous phase volumes used at this stage define the volume ratio. This electrode was covered by a thick layer of 100 µL of the organic solution at equilibrium and immersed in excess of aqueous solution. Ohmic drop compensation was manually set in order to obtain a peak-to-peak potential difference of 100 mV or less, since 90 mV is expected for reversible processes in this setup [38,39].

4. Results and discussion

Results and their discussion are presented in four sections. First, the relevance and physical meaning of the external applied potential when one of the two serial interfaces is at its half-wave potential. Furthermore, the equations to calculate the half-wave potential as a function of pH are discussed without taking into account IP and NIES. In the second and third section, discussions of the effects of introducing these phenomena are presented, and in the last section, the theoretical approach is validated by voltammetric experiments for Tylosin A transfer.

4.1. The significance of the half-wave potential

The equations developed in the theory section provide two different analytical expressions for the external applied potential: in the first case, the Eqs. (29) and (30), represent the external applied potential when the S|L interface is at its half-wave potential, while the other couple of expressions (Eqs. (34) and (35)) yield the external applied potential when the L|L interface is at its half-wave potential. Since the species that defines the current

response for this coupled process is either Ox or the weak base (in its protonated or deprotonated form), only one of these equations will be of interest for each set of experimental conditions, depending on the initial concentration ratio between the weak base and redox species. The half-wave potential, $\Delta\phi_{1/2}$, of the FPT-ET reactions is defined here as the external applied potential when the interface that involves the limiting charge transfer reaction is at its half-wave potential $\left(\Delta_{\mathrm{O}}^{\mathrm{W}}\phi_{1/2}\ \text{or}\ \Delta_{\mathrm{O}}^{\mathrm{S}}\phi_{1/2}\right)$. Mathematically:

$$\Delta\phi_{1/2}=\begin{cases}\Delta_{\mathrm{O}}^{\mathrm{S}}\phi\left(\Delta_{\mathrm{O}}^{\mathrm{W}}\phi_{1/2}\right)-\Delta_{\mathrm{O}}^{\mathrm{W}}\phi_{1/2} & \text{if}\ \ \sqrt{D^{\mathrm{W}}}c_{\mathrm{B,tot}}^{\mathrm{init}}\le\sqrt{D_{\mathrm{Ox}}^{\mathrm{O}}}c_{\mathrm{Ox}}^{\mathrm{init}}\\ \Delta_{\mathrm{O}}^{\mathrm{S}}\phi_{1/2}-\Delta_{\mathrm{O}}^{\mathrm{W}}\phi\left(\Delta_{\mathrm{O}}^{\mathrm{S}}\phi_{1/2}\right) & \text{if}\ \ \sqrt{D^{\mathrm{W}}}c_{\mathrm{B,tot}}^{\mathrm{init}}>\sqrt{D_{\mathrm{Ox}}^{\mathrm{O}}}c_{\mathrm{Ox}}^{\mathrm{init}}\end{cases} \tag{36}$$

The reason for this definition and its physical meaning will be discussed below.

For a single ion transfer or electron transfer reaction which is electrochemically reversible and diffusion controlled, the half-wave potential can be assumed to be equal to the mid-peak potential, E_{mid}, calculated as the arithmetic mean of the forward and backward peak potentials in a cyclic voltammogram, $E_{mid}=\frac{1}{2}\left(E_{peak}^{forward\ scan}+E_{peak}^{backward\ scan}\right)$ [66]. In the case of coupled charge transfer reactions, this is not necessarily true, since voltammograms show slight asymmetries [38,39,59,67] that shift the value of the mid-peak potential away from the half-wave potential. The deviation from the behaviour of a reversible diffusion-controlled electrochemical process in a single polarized interface can be explained by the variation in the Galvani potential difference at both interfaces with external applied potential at two polarized interfaces setup [39,58,67,68]. In order to analyse this difference, four different sets of conditions were selected to compare these magnitudes. Fig. 2 shows $\Delta\phi_{1/2}$

according to Eq. (36) and E_{mid} obtained from finite difference simulations as described in Ref. [38] as a function of pH at different volume ratios. The observed dependence of potential values with pH, has been already discussed in previous article [38]. In general, for low pH values, HB^+ is the predominant species and its concentration throughout the phase does not depend on the volume ratio, however, for higher pH values, the weak base is deprotonated and its initial concentration in the organic phase decreases as the volume ratio increases. This change in concentrations produces a peak potential shift. The developed analytical expressions for $\Delta\phi_{1/2}$ very accurately represent the pH dependence of E_{mid} in all experimental conditions. There is, however, a slight difference between these values. This difference is independent of experimental conditions and satisfies $\left|E_{mid} - \Delta\phi_{1/2}\right| \approx 4\,\mathrm{mV}$ in all cases, as previously reported for two polarized interfaces setup by Samec et al. [67]. In fact, although $\Delta\phi_{1/2}$ cannot be easily obtained from voltammetry experiments, the finite difference simulations allow the determination of its value. It is the external applied potential in which the concentration at the interface of the limiting reactant and formed product are the same (considering all diffusion coefficients are the same). When plotting this value instead of E_{mid}, they exactly agree with the results obtained from Eq. (36). These results validate both numerical simulations and theoretical equations.

The half-wave potential is expected to be a continuous function. Thus, in order to define the domain of each piece of Eq. (36), the right hand terms of Eqs. (29) and (34) are equalled. After simplifying and rearranging, the following expression is obtained:

$$\sqrt{D_{\mathrm{Ox}}^{\mathrm{O}}}c_{\mathrm{Ox}}^{\mathrm{init}}=\sqrt{D^{\mathrm{W}}}c_{\mathrm{B}}^{\mathrm{a}}\left(\frac{1+\sqrt{\frac{D^{\mathrm{O}}}{D^{\mathrm{W}}}}\alpha_{\mathrm{B}}K_{\mathrm{D,B}}^{'}}{1+r\alpha_{\mathrm{B}}K_{\mathrm{D,B}}^{'}}\right) \tag{37}$$

which can be expressed as:

$$\sqrt{D_{\mathrm{Ox}}^{\mathrm{O}}}c_{\mathrm{Ox}}^{\mathrm{init}}=\sqrt{D^{\mathrm{W}}}c_{\mathrm{B,tot}}^{\mathrm{init}} \tag{38}$$

thus, the criterion to select Eqs. (29) or (34) to calculate $\Delta\phi_{1/2}$ is defined as specified in Eq. (36).

The convenience of defining the half-wave potential in this way is illustrated when experimental conditions are gradually modified from an excess of one species towards an excess of the other. Adequate experimental conditions for illustrative chemical systems were selected to achieve this, and results are shown in Fig. 3. In these two panels, it is shown that $\Delta\phi_{1/2}$ represents the maximum between $\left[\Delta_{\mathrm{O}}^{\mathrm{S}}\phi_{1/2}-\Delta_{\mathrm{O}}^{\mathrm{W}}\phi\left(\Delta_{\mathrm{O}}^{\mathrm{S}}\phi_{1/2}\right)\right]$ and $\left[\Delta_{\mathrm{O}}^{\mathrm{S}}\phi\left(\Delta_{\mathrm{O}}^{\mathrm{W}}\phi_{1/2}\right)-\Delta_{\mathrm{O}}^{\mathrm{W}}\phi_{1/2}\right]$, meaning the minimum between the two possible changes in Gibbs free energy, and exactly follows the trend in E_{mid}. This confirms, firstly, that the initial concentrations define whether the FTP or the ET process limits the charge transfer, and secondly, that $\Delta\phi_{1/2}$, as defined above, can be straightforwardly estimated from cyclic voltammetry experiments by measuring peak potentials for a wide variety of experimental conditions.

Although the break points in both plots of Fig. 3, would only be of academic interest, they can be easily calculated as follows:

$$pH = -\log\left\{\frac{\sqrt{D_{Ox}^{O}}\,c_{Ox}^{init}\left[K_{a,HB^+}^{W'}\left(1+rK_{D,B}^{'}\right)\right]-\sqrt{D^{W}}\,c_{B}^{a}\left[K_{a,HB^+}^{W'}\left(1+\sqrt{\frac{D^{O}}{D^{W}}}K_{D,B}^{'}\right)\right]}{\sqrt{D^{W}}\,c_{B}^{a}-\sqrt{D_{Ox}^{O}}\,c_{Ox}^{init}}\right\} \quad (39)$$

4.2 Effect of ion pairing on the half-wave potential

Only ion pairs formed in the organic phase were considered in the model, since dielectric constants in organic solvents can be much lower than in water [62,69–71]. Three ion pairs were identified as the most relevant: the first is formed by the ions in the organic supporting electrolyte: KY, and the others are formed by each of these ions and the electrochemical reaction products: $KRed$ and HBY. There is no need to take into account the formation of $HBRed$ ion pair, since the thick film setup prevents the diffusion layers of these ions from overlapping [59].

The organic supporting electrolyte concentration becomes a critical variable when ion pairs are involved in the electrochemical process. In fact, performing experiments with different concentrations of supporting electrolyte is a very straightforward strategy to evaluate ion pair formation [26]. Fig. 4a and Fig. 4b show the effect of ion pairing on the half-wave potential for different sets of formation constants. Fig. 4a corresponds to conditions for which the formation of KY ion pair is negligible, while Fig. 4b corresponds to conditions for which KY is present. As shown by the orange lines in both plots, when no ion pairs are formed, or only KY presents a significant formation constant, no variation of

$\Delta\phi_{1/2}$ is observed, since the supporting electrolyte does not directly affect the electrochemical reaction.

The slope of the curves in Figs. 4a and 4b for high supporting electrolyte concentrations can be directly inferred by means of the analysis of the expression for $\Delta\phi_{1/2}$ (Eq. (36)). By rearranging Eqs. (30) and (35), they can be reduced to:

$$\Delta\phi_{1/2} = constant + \frac{RT}{F}\ln\left[\left(1+K'_{\mathrm{KRed}}\alpha_{\mathrm{SE}}c^{\mathrm{O}}_{\mathrm{SE}}\right)\left(1+K'_{\mathrm{HBY}}\alpha_{\mathrm{SE}}c^{\mathrm{O}}_{\mathrm{SE}}\right)\right] \quad (40)$$

where the *constant* parameter is independent of $c^{\mathrm{O}}_{\mathrm{SE}}$ and ion pair formation constants. This shows that the effective formation constant of KRed and HBY ion pairs have the exact same effect on $\Delta\phi_{1/2}$, independently on the initial concentrations of Ox and HBX. As the argument of the logarithm in Eq. (40) is larger than unity, this influence always favours the FPT-ET reaction, shifting $\Delta\phi_{1/2}$ towards values that are more positive. This effect is analogous to the facilitated ion transfer commonly described in ITIES and the electrochemical-chemical mechanism described for electron transfer reactions combined in the same experimental setup [38].

For the cases corresponding to Fig. 4a, i.e. when the entirety of the organic supporting electrolyte is dissociated, $\alpha_{\mathrm{SE}} = 1$, and this expression is reduced to:

$$\Delta\phi_{1/2} = constant + \frac{RT}{F}\ln\left[\left(1+K'_{\mathrm{KRed}}c^{\mathrm{O}}_{\mathrm{SE}}\right)\left(1+K'_{\mathrm{HBY}}c^{\mathrm{O}}_{\mathrm{SE}}\right)\right] \quad (41)$$

From it, the slopes of the curves in Fig. 4a can be rationalized: the blue line, for which only the formation of KRed ion pair is significant, presents a linear region for which the slope is

59 mV per decade. In this situation, only the factor $1+K'_{\mathrm{KRed}}c^{\mathrm{O}}_{\mathrm{SE}}$ in Eq. (41) is different from unity and thus the factor RT/F yields the observed slope. This effect is the same for the other individual ion pair, HBY, (not shown in the plot). When both ion pairs are present, their effects accumulate, yielding a linear slope of 118 mV per decade present in the red line of Fig. 4a.

On the other hand, when the supporting electrolyte is not fully dissociated, the limiting behaviour of α_{SE} as $c^{\mathrm{o}}_{\mathrm{SE}}$ increases was shown in previous work to be $\alpha_{\mathrm{SE}}=\left(K'_{\mathrm{SE}}c^{\mathrm{o}}_{\mathrm{SE}}\right)^{-\frac{1}{2}}$ [26]. By replacing this expression in Eq. (41), the following limiting equation can be found:

$$\Delta\phi_{1/2}=constant+\frac{RT}{F}\ln\left[\left(1+\frac{K'_{\mathrm{KRed}}}{\sqrt{K'_{\mathrm{SE}}}}\left(c^{\mathrm{o}}_{\mathrm{SE}}\right)^{\frac{1}{2}}\right)\left(1+\frac{K'_{\mathrm{HBY}}}{\sqrt{K'_{\mathrm{SE}}}}\left(c^{\mathrm{o}}_{\mathrm{SE}}\right)^{\frac{1}{2}}\right)\right] \tag{42}$$

In this expression, the exponent of $c^{\mathrm{o}}_{\mathrm{SE}}$ is halved with respect to Eq. (40), which explains that in Fig. 4b, the slopes of the curves are also halved with respect to their analogues in Fig. 4a, i.e. 29.5 mV for only one ion pair (blue line) and 59 mV for both ion pairs at the same time (red line). This great shift in $\Delta\phi_{1/2}$ is explained by the substantial change in α_{SE}, as shown in Fig. 4c, which translates into a lower proportion of K^+ and Y^- ions available for ion pairing.

The magnitude of the ion pair formation constants also plays an important role in defining $\Delta\phi_{1/2}$. Fig. 5 compares three different sets of non-negligible constants. In all cases, the linear sections present a slope of 59 mV, as discussed above. The first line, in red, shows

the same data as the red line in Fig. 4b. Taking this situation as a reference, when the ion pair formation constant that corresponds to one of the products is increased, the same behavior occurs at lower supporting electrolyte concentrations. Conversely, when the supporting electrolyte ion pair formation constant is increased, the inverse effect is observed. $\Delta\phi_{1/2}$ greatly decreases in this case because the dissociated fraction decreases (Fig. 5b). The analysis presented above yields two important conclusions: firstly, in order to assess the formation of ion pairs in the organic phase it is important to carry out experiments for different concentrations of supporting electrolyte. Secondly, in the thick-film configuration, it is impossible to discern from $\Delta\phi_{1/2}$ determinations alone, whether the product in the S|L interface (Red^-) or the L|L interface (HB^+) is forming ion pairs with the supporting electrolyte.

4.3 Effect of ion pairing and non-ideality in electrolyte solutions on the half-wave potential.

This section analyses the effect of realistic activity coefficients together with the ion pairing effects reviewed above. Fig. 6 compares $\Delta\phi_{1/2}$ for ideal and non-ideal electrolyte solutions, for the same sets of ion pair formation constants as in Fig. 5a. No significant differences in the shape of these plots were observed with changes in pH, besides the expected shift towards negative potentials as pH rises (data not shown). A great discrepancy between a system that behaves ideally and non-ideal electrolyte solutions is observed for very high concentrations of supporting electrolyte. Nevertheless, it is worth noting that for typical values of $\log\left(c_{\mathrm{SE}}^{\mathrm{O}}\right) \leq -1.0$, the difference in $\Delta\phi_{1/2}$ for ideal and non-ideal electrolytes is always less than 10 mV, which is a reasonably small difference. This

would allow, in principle, to disregard the effect of the activity coefficients on the half-wave potential without substantial negative effects, as long as some care is taken in order to minimize this effect.

The abrupt change in $\Delta\phi_{1/2}$ observed as $\log\left(c_{\mathrm{SE}}^{\mathrm{O}}\right)$ increases above −1.0 can be attributed to the effective ion pair formation constants. These values depend on the activity coefficients as described by Eqs. (5)-(7). To calculate ion activity coefficients Eqs. (1) and (2), considering $a_\alpha = b_{+,\alpha} = b_{-,\alpha}$ was used. For neutral ion pairs, a different expression, Eq. (3) was selected [26]. The particular parameters used in Fig. 6, for which $V^{\mathrm{intr}} < V^0$, imply that $\gamma_{\mathrm{KY}}^{\mathrm{o}}$ decreases as ionic strength (given by $c_{\mathrm{SE}}^{\mathrm{O}}$) increases, while $\gamma_{\mathrm{K}^+}^{\mathrm{O}}$ and $\gamma_{\mathrm{Y}^-}^{\mathrm{O}}$ remain bounded. In consequence, the factor $\gamma_{\mathrm{K}^+}^{\mathrm{O}}\gamma_{\mathrm{Y}^-}^{\mathrm{O}}\left(\gamma_{\mathrm{KY}}^{\mathrm{O}}\right)^{-1}$ in the expression for $K_{\mathrm{SE}}^{'}$ grows and the dissociated fraction of supporting electrolyte sharply decreases as $\log\left(c_{\mathrm{SE}}^{\mathrm{O}}\right)$ increases, greatly limiting the formation of KRed and HBY ion pairs. Thus, $\Delta\phi_{1/2}$ reverts to values expected for much smaller supporting electrolyte concentration under ideal conditions.

4.4 Validation of the model from experimental results

In the set of performed experiments, concentrations of supporting electrolyte in the organic phase were within typical values. In particular, a concentration of supporting electrolyte in the organic phase of $\log\left(c_{\mathrm{SE}}^{\mathrm{O}}\right) = -1.45$, and a bufferized aqueous phase between $\mathrm{pH} = 3.5 \pm 0.1$ (acetate buffer) and $\mathrm{pH} = 6.7 \pm 0.1$(phosphate buffer) were

employed. These experiments, shown in Fig. 7, clearly verify that E_{mid} remains constant at low pH values for two different volume ratios. Conversely, at high pH values, a shift towards negative values is observed as the volume ratio increases. Reproducibility was assessed with five repetitions of the same experiment (Fig. B1 Supplementary Material).

To show the complete landscape, two different volume ratios were chosen: $r = 1.00$ and $r = 0.125$, and several voltammetric experiments were performed at different pH values of the aqueous phase. Figs. 8a and 8b show E_{mid} from electrochemical experiments as a function of pH plotted as hollow points. These values were determined from cyclic voltammetry (CV) and square wave voltammetry (SWV) as detailed in Table B1 in the Supplementary Material. In continuous lines in the same figures, results obtained from the theory (Eq. (36)), without taking into account IP or NIES are shown. These values were adjusted to the experimental data only by the addition of an offset. The offset parameter can be associated to the formal reduction potential of the redox probe in the organic phase ($\Delta_{\mathrm{O}}^{\mathrm{S}}\phi^{\mathrm{o'}}$) which is unknown, the reference electrode potential difference and possibly IP effect.

Data obtained from CV and SWV show the same tendency, and are in very good agreement with the theoretical results. Consequently, experiments confirm that E_{mid} depends on volume ratio and pH as predicted by the proposed model.

Finally, it should be mentioned that all experimental current-potential profiles presented here show a peak-to-peak potential difference of around or less than 100 mV which is close to the characteristic peak-to-peak potential difference of 90 mV previously predicted from simulations [38,39], this is an additional indication of the good agreement between the model and the experiments for FPT-ET reactions.

5. Conclusion

Analytical expressions for $\Delta_{\mathrm{O}}^{\mathrm{S}}\phi_{1/2} - \Delta_{\mathrm{O}}^{\mathrm{W}}\phi\left(\Delta_{\mathrm{O}}^{\mathrm{S}}\phi_{1/2}\right)$ and $\Delta_{\mathrm{O}}^{\mathrm{S}}\phi\left(\Delta_{\mathrm{O}}^{\mathrm{W}}\phi_{1/2}\right) - \Delta_{\mathrm{O}}^{\mathrm{W}}\phi_{1/2}$ were developed for the thick-film setup. It was shown that these magnitudes are relevant in experiments, since they are directly correlated to the mid-peak potential in cyclic voltammetry and the peak potential in square-wave voltammetry. The effects of ion pairing and non ideality of the electrolyte solutions were explicitly incorporated into these expressions. This allows showing that in order to assess the formation of ion pairs in the system, it is important to carry out experiments for different concentrations of organic supporting electrolyte, which facilitates the charge transfer processes. However, this does not allow to distinguish which of the ions in the supporting electrolyte is responsible for this effect. On the other hand, it was shown that non-ideality of electrolyte solutions has a lower impact on the half-wave potential for typical experimental conditions. Experimental data from cyclic voltammetry and square wave voltammetry show exactly the same trend and are in good agreement with those obtained from analytical expressions. In addition, these results match perfectly with those obtained by finite difference simulations. In this manner, the integrated theoretical-experimental approach provides some experimental guidelines related to the range of validity of thermodynamic parameters, acquired from electrochemical experiments, including the effect of ion pairing and non-ideal electrolyte solutions.

Acknowledgements

R.A.F. and S.A.D. are Researchers from Consejo Nacional de Investigaciones Científicas y Tecnológicas (CONICET). F.M.Z., thanks CONICET for the fellowships granted. Financial support from CONICET, Secretaría de Ciencia y Tecnología de la Universidad Nacional de Córdoba (SECyT-UNC) and Fondo para la Investigación Científica y Tecnológica (FONCyT) PICT-2012-1820 are gratefully acknowledged.

References

[1] Z. Yoshida, H. Freiser, J. Electroanal. Chem. 162 (1984) 307–319.

[2] D. Homolka, V. Mareček, Z.Z. Samec, K. Baše, H.H. Wendt, J. Electroanal. Chem. 163 (1984) 159–170.

[3] F. Reymond, G. Steyaert, P.-A. Carrupt, B. Testa, H.H. Girault, Helv. Chim. Acta 79 (1996) 101–117.

[4] F. Reymond, P.-F. Brevet, P.-A. Carrupt, H.H. Girault, J. Electroanal. Chem. 424 (1997) 121–139.

[5] Z. Ding, F. Reymond, P. Baumgartner, D.J. Fermín, P.-F. Brevet, P. Carrupt, H.H. Girault, Electrochim. Acta 44 (1998) 3–13.

[6] Y. Kubota, H. Katano, K. Maeda, M. Senda, Electrochim. Acta 44 (1998) 109–116.

[7] Z. Samec, J. Langmaier, A. Trojánek, E. Samcová, J. Málek, Anal. Sci. 14 (1998) 35–41.

[8] S. Sawada, T. Osakai, Phys. Chem. Chem. Phys. 1 (1999) 4819–4825.

[9] F. Reymond, P.-A. Carrupt, B. Testa, H.H. Girault, Chem. Eur. J. 5 (1999) 39–47.

[10] A.I. Azcurra, L.M. Yudi, A.M. Baruzzi, J. Electroanal. Chem. 461 (1999) 194–200.

[11] F. Reymond, V. Chopineaux-Courtois, G. Steyaert, G. Bouchard, P.-A. Carrupt, B. Testa, H.H. Girault, J. Electroanal. Chem. 462 (1999) 235–250.

[12] W. Wickler, A. Mönner, E. Uhlemann, S. Wilke, H. Müller, J. Electroanal. Chem. 469 (1999) 91–96.

[13] Y. Liu, E. Wang, J. Chem. Soc. Faraday Trans. I 83 (1987) 2993–2999.

[14] M. Senda, Y. Kubota, H. Katano, in:, Liq. Interfaces Chem. Biol. Pharm. Appl., 2001, pp. 683–698.

[15] Y. Kubota, H. Katano, M. Senda, Anal. Sci. 17 (2001) 65–70.

[16] R.A. Fernández, S.A. Dassie, J. Electroanal. Chem. 585 (2005) 240–249.

[17] J.I. Garcia, R.A. Iglesias, S.A. Dassie, J. Electroanal. Chem. 586 (2006) 225–236.

[18] J.I. Garcia, R.A. Fernández, A.J. Ruggeri, S.A. Dassie, J. Electroanal. Chem. 594 (2006) 80–88.

[19] M. Rimboud, C. Elleouet, F. Quentel, J.-M. Kerbaol, M. L'Her, J. Electroanal. Chem. 622 (2008) 233–237.

[20] R.A. Fernández, M.I. Velasco, L.I. Rossi, S.A. Dassie, J. Electroanal. Chem. 650 (2010) 47–54.

[21] J.I. Garcia, M.B. Oviedo, S.A. Dassie, J. Electroanal. Chem. 645 (2010) 1–9.

[22] M. Velický, K.Y. Tam, R.A.W. Dryfe, J. Electroanal. Chem. 683 (2012) 94–102.

[23] M. Velický, K.Y. Tam, R.A.W. Dryfe, Anal. Chem. 84 (2012) 2541–2547.

[24] H. Doe, K. Yoshioka, T. Kitagawa, J. Electroanal. Chem. 324 (1992) 69–78.

[25] S.A. Dassie, J. Electroanal. Chem. 728 (2014) 51–59.

[26] F. Vega Mercado, F.M. Zanotto, R.A. Fernández, S.A. Dassie, J. Electroanal. Chem. 774 (2016) 111–121.

[27] F. Vega Mercado, J.M. Ovejero, R.A. Fernández, S.A. Dassie, J. Electroanal. Chem. 765 (2016) 100–104.

[28] S.A. Dassie, J. Electroanal. Chem. 578 (2005) 159–170.

[29] S.A. Dassie, J. Electroanal. Chem. 585 (2005) 256–268.

[30] E. Torralba, J. a Ortuño, A. Molina, C. Serna, F. Karimian, Anal. Chim. Acta 826 (2014) 12–20.

[31] F. Vega Mercado, J.M. Ovejero, F.M. Zanotto, M.R. Serial, M.I. Velasco, R.A. Fernández, R.H. Acosta, S.A. Dassie, J. Electroanal. Chem. 791 (2017) 64–74.

[32] L.M. Yudi, A.M. Baruzzi, J. Electroanal. Chem. 328 (1992) 153–164.

[33] K. Kontturi, L. Murtomäki, J. Pharm. Sci. 81 (1992) 970–975.

[34] L.M. Yudi, A.M. Baruzzi, V.M. Solis, J. Electroanal. Chem. 360 (1993) 211–219.

[35] S.A. Dassie, L.M. Yudi, A.M. Baruzzi, Electrochim. Acta 40 (1995) 2953–2959.

[36] F. Reymond, G. Steyaert, A. Pagliara, P. Carrupt, B. Testa, H.H. Girault, Helv. Chim. Acta 79 (1996) 1651–1669.

[37] F. Reymond, G. Steyaert, P.-A. Carrupt, B. Testa, H.H. Girault, J. Am. Chem. Soc. 118 (1996) 11951–11957.

[38] F.M. Zanotto, R.A. Fernández, S.A. Dassie, Electrochim. Acta 258 (2017) 727–734.

[39] F.M. Zanotto, R.A. Fernández, S.A. Dassie, J. Electroanal. Chem. 784 (2017) 25–32.

[40] D. Fraenkel, Mol. Phys. 108 (2010) 1435–1466.

[41] D. Fraenkel, J. Phys. Chem. B 115 (2011) 557–568.

[42] D. Fraenkel, J. Phys. Chem. B 116 (2012) 3603–3612.

[43] D. Fraenkel, J. Chem. Theory Comput. 11 (2015) 178–192.

[44] D. Fraenkel, J. Chem. Theory Comput. 11 (2015) 193–204.

[45] F.A. Long, W.F. McDevit, Chem. Rev. 51 (1952) 119–169.

[46] W.F. McDevit, F. a Long, J. Am. Chem. Soc. 74 (1952) 1773–1777.

[47] Y. Marcus, J. Mol. Liq. 123 (2006) 8–13.

[48] Y. Marcus, Ions in Solution and Their Solvation, John Wiley & Sons, Inc, Hoboken, New Jersey, 2015.

[49] F.J. Millero, R.W. Curry, W. Drost-Hansen, J. Chem. Eng. Data 14 (1969) 422–425.

[50] F.J. Millero, Chem. Rev. 71 (1971) 147–176.

[51] J.-F. Côté, J.E. Desnoyers, J.-C. Justice, J. Solution Chem. 25 (1996) 113–134.

[52] Y. Marcus, H. Donald, B. Jenkins, L. Glasser, J. Chem. Soc. Dalt. Trans. (2002) 3795–3798.

[53] Y. Marcus, G. Hefter, Chem. Rev. 104 (2004) 3405–3452.

[54] Y. Marcus, J. Solution Chem. 37 (2008) 1071–1098.

[55] D.R. Lide, CRC Handbook of Chemistry and Physics, 84th Ed., CRC Press, Boca Raton, FL, 2003.

[56] Y. Marcus, The Properties of Solvents, John Wiley & Sons Ltd, New York, 1998.

[57] Margaret Robson Wright, An Introduction to Aqueous Electrolyte Solutions, John Wiley & Sons Ltd, 2007.

[58] A. Molina, C. Serna, J. Gonzalez, J.A. Ortuño, E. Torralba, Phys. Chem. Chem. Phys. 11 (2009) 1159–1166.

[59] M. Zhou, S. Gan, L. Zhong, X. Dong, J. Ulstrup, D. Han, L. Niu, Phys. Chem. Chem. Phys. 14 (2012) 3659.

[60] A.J. Bard, C.R. Faulkner, Electrochemical Methods, Fundamentals and Applications, 2nd ed., John Wiley & Sons, New York, 2001.

[61] F. Reymond, G. Lagger, P.-A. Carrupt, H.H. Girault, J. Electroanal. Chem. 451 (1998) 59–76.

[62] T. Wandlowski, V. Mareček, Z. Samec, Electrochim. Acta 35 (1990) 1173–1175.

[63] A. Sabela, V. Mareček, Z. Samec, R. Fuoco, Electrochim. Acta 37 (1992) 231–235.

[64] S.M. Ulmeanu, H.J. Lee, D.J. Fermín, H.H. Girault, Y. Shao, Electrochem. Commun. 3 (2001) 219–223.

[65] A.M. Baruzzi, H. Wendt, J. Electroanal. Chem. 279 (1990) 19–30.

[66] F. Scholz, ed., Electroanalytical Methods: Guide to Experiments and Applications, 2nd editio, Springer-Verlag, 2010.

[67] Z. Samec, A. Trojánek, J. Langmaier, E. Samcová, J. Electroanal. Chem. 481 (2000) 1–6.

[68] A. Molina, C. Serna, J.A. Ortuno, E. Torralba, Annu. Reports Sect. C Phys. Chem. 108 (2012) 126–176.

[69] Y. Marcus, G. Hefter, Chem. Rev. 106 (2006) 4585–4621.

[70] Z. Samec, V. Mareček, M.P. Colombini, J. Electroanal. Chem. 257 (1988) 147–154.

[71] T. Kakiuchi, Anal. Chem. 68 (1996) 3658–3664.

[72] Z. Samec, Pure Appl. Chem. 76 (2004) 2147–2180.

[73] Y. Marcus, J. Solution Chem. 33 (2004) 549–559.

[74] Y. Marcus, J. Solution Chem. 34 (2005) 317–331.

[75] J.W. McFarland, C.M. Berger, S.A. Froshauer, S.F. Hayashi, S.J. Hecker, B.H. Jaynes, M.R. Jefson, B.J. Kamicker, C.A. Lipinski, K.M. Lundy, C.P. Reese, C.B. Vu, J. Med. Chem. 40 (1997) 1340–1346.

Figure captions

Fig.1: Schematic representation of the possible mechanisms involving electron transfer at the solid|liquid interface, ion transfer at the liquid|liquid interface and ion pair formation. (a) Simple mechanism. (b) Facilitated mechanism.

Fig.2: Half-wave potential, $\Delta\phi_{1/2}$ (*full lines*), and mid-peak potential, E_{mid} (*open circles*), as a function of pH at different organic to aqueous volume ratios for the thick-film setup. For the simulations with weak base is in excess: $c_{\mathrm{B}}^{\mathrm{a}} = 0.1\,\mathrm{M}$, $c_{ox}^{\mathrm{init}} = 0.0001\,\mathrm{M}$ (—) $r = 0.1$ and (—) $r = 10$. For the redox probe in excess $c_{\mathrm{B}}^{\mathrm{a}} = 0.0001\,\mathrm{M}$, $c_{ox}^{\mathrm{init}} = 0.1\,\mathrm{M}$ (—) $r = 0.1$ and (—) $r = 10$. Other simulation parameters: $\mathrm{p}K_{\mathrm{a,HB^+}}^{\mathrm{W}} = 8.00$, $K_{\mathrm{D,B}} = 1000$, $\Delta_{\mathrm{o}}^{\mathrm{w}}\phi_{\mathrm{HB^+}}^{\circ} = 0.100\mathrm{V}$, $\Delta_{\mathrm{o}}^{\mathrm{w}}\phi_{\mathrm{H^+}}^{\circ} = 0.550\mathrm{V}$ all diffusion coefficients equal to $1\times10^{-5}\mathrm{cm^2s^{-1}}$.

Fig.3: Comparative dependence of mid-peak potential obtained from finite element simulations (●) and half-wave potential obtained from theoretical equations as a function of pH. $\Delta\phi_{1/2}$ (—); $\left[\Delta_{\mathrm{O}}^{\mathrm{S}}\phi_{1/2} - \Delta_{\mathrm{O}}^{\mathrm{W}}\phi\left(\Delta_{\mathrm{O}}^{\mathrm{S}}\phi_{1/2}\right)\right]$ according to Eq.(29) (—); $\left[\Delta_{\mathrm{O}}^{\mathrm{S}}\phi\left(\Delta_{\mathrm{O}}^{\mathrm{W}}\phi_{1/2}\right) - \Delta_{\mathrm{O}}^{\mathrm{W}}\phi_{1/2}\right]$ according to Eq.(34) (—). (a) $c_{\mathrm{B}}^{\mathrm{a}} = 0.1\,\mathrm{M}$, $c_{ox}^{\mathrm{init}} = 0.001\,\mathrm{M}$, $r = 1\times10^{3}$; (b) $c_{\mathrm{B}}^{\mathrm{a}} = 0.001\,\mathrm{M}$, $c_{ox}^{\mathrm{init}} = 0.1\,\mathrm{M}$, $r = 1\times10^{-3}$. All other simulation parameters are the same as in Fig. 2.

Fig.4: Effect of supporting electrolyte concentration in the organic phase on the global half-wave potential when ion pairing is considered. Panel (a) corresponds to a negligible KY ion pair formation constant ($K_{\mathrm{SE}} = 2\times10^{-8}$), while for panel (b), $K_{\mathrm{SE}} = 2\times10^{3}$. Simulation parameters: $K_{\mathrm{HBY}} = 1\times10^{-8}$ and $K_{\mathrm{KRed}} = 1\times10^{-8}$ (—), $K_{\mathrm{HBY}} = 1\times10^{-8}$ and $K_{\mathrm{KRed}} = 1\times10^{3}$ (—), $K_{\mathrm{HBY}} = 1\times10^{3}$ and $K_{\mathrm{KRed}} = 1\times10^{3}$ (—). Other simulation parameters: $\mathrm{p}K_{\mathrm{a,HB^+}}^{\mathrm{W}} = 8.36$, $K_{\mathrm{D,B}} = 125$, $\Delta_{\mathrm{o}}^{\mathrm{w}}\phi_{\mathrm{HB^+}}^{\circ} = 0.100\mathrm{V}$, $\Delta_{\mathrm{o}}^{\mathrm{w}}\phi_{\mathrm{H^+}}^{\circ} = 0.550\mathrm{V}$ all diffusion coefficients equal to $1\times10^{-5}\mathrm{cm^2s^{-1}}$.

Panel (c): Supporting electrolyte concentration dependence of KY dissociation degree (α_{SE}), corresponding to simulations in panel (b).

Fig.5: (a) Effect of supporting electrolyte concentration in the organic phase on the global half-wave potential when ion pairing is considered. Simulation parameters: $K_{SE} = 2\times10^{3}$ and $K'_{KRed} = 1\times10^{3}$ (—), $K_{SE} = 2\times10^{3}$ and $K'_{KRed} = 1\times10^{5}$ (—), $K_{SE} = 2\times10^{5}$ and $K'_{KRed} = 1\times10^{3}$ (—). All other parameters are the same as in Fig. 4. **(b)** Supporting electrolyte concentration dependence of KY dissociated fraction. $K_{SE} = 2\times10^{3}$ (—), $K_{SE} = 2\times10^{5}$ (—).

Fig.6: Effect of supporting electrolyte concentration in the organic phase on the global half-wave potential when both IP and NIES are considered. Dashed lines correspond to the same lines as in Fig. 5a. Continuous lines simulation parameters: $K_{SE} = 2\times10^{3}$ and $K'_{KRed} = 1\times10^{3}$ (—), $K_{SE} = 2\times10^{3}$ and $K'_{KRed} = 1\times10^{5}$ (—), $K_{SE} = 2\times10^{5}$ and $K'_{KRed} = 1\times10^{3}$ (—). $\varepsilon_{w} = 78.38$ [42], $\varepsilon_{1,2-DCE} = 10.36$ [72], $\sigma_{w} = 0.99704\,\mathrm{g\,cm^{3}}$ [42], $\sigma_{1,2-DCE} = 1.2458\,\mathrm{g\,cm^{3}}$ [72], $\kappa_{T,1,2-DCE} = 0.846\,\mathrm{GPa^{-1}}$ [55], $V^{intr}_{KY} = 380\,\mathrm{cm^{3}mol^{-1}}$, $V^{0}_{KY} = 450\,\mathrm{cm^{3}mol^{-1}}$, $V^{intr}_{HBY} = V^{intr}_{KRed} = 250\,\mathrm{cm^{3}mol^{-1}}$ and $V^{0}_{HBY} = V^{0}_{KRed} = 280\,\mathrm{cm^{3}mol^{-1}}$ [47,52,54,73,74]. All other parameters are the same as in Fig. 4.

Fig.7: Experimental cyclic voltammograms at $0.100\,\mathrm{Vs^{-1}}$. Organic phase: TPADCC 0.038 M and TCNQ 0.23 mM in 1,2-DCE. Aqueous phase: Acetate or phosphate buffer solution 0.50 M and Tylosin A tartrate 3.0 mM. Experimental conditions: *r* = 0.125 and pH = 3.5 (—), *r* = 0.125 and pH = 6.7 (—), *r* = 1.00 and pH = 3.5 (—), *r* = 1.00 and pH = 6.7 (—).

Fig.8: Experimental data (*hollow points*) as a function of pH for *r* = 1.00 (—) and *r* = 0.125 (—). All other experimental conditions are the same as in Fig. 7. Continuous lines represent the adjusted $\Delta\phi_{1/2}$ according to Eq. (36) using: $\mathrm{p}K^{W}_{a,HB^{+}} = 7.73$ [75] and $\log\left(K_{D,B}\right) = 3.1$ [20] (a) Mid-peak potential from cyclic voltammetry and (b) Peak potential from square wave voltammetry.

Table 1: principal symbols used in this work.

Symbol	Meaning	Units
$c_i^{\alpha}(x, \Delta_{\mathrm{O}}^{\mathrm{S}}\phi_{1/2})$	Concentration of the *i* species in phase α at x position at the time when the potential at the S|L interface is equal to its half-wave potential.	mM
$c_i^{\alpha}(x, \Delta_{\mathrm{O}}^{\mathrm{W}}\phi_{1/2})$	Concentration of the *i* species in phase α at x position at the time when the potential at the L|L interface is equal to its half-wave potential.	mM
$c_{\mathrm{Red}^-}^{\mathrm{O}}(0,t)$	Concentration of the reduced species at the solid electrode surface (x=0) at any time.	mM
$c_{\mathrm{HB}^+}^{\mathrm{O}}(L,t)$	Concentration of HB^+ species at the L|L interface (x=L) at any time.	mM
$c_{\mathrm{Ox}}^{\mathrm{init}}$	Initial concentration of the oxidized species in the organic phase.	mM
$c_{\mathrm{B}}^{\mathrm{O}}$	Initial concentration of the weak base in the organic phase **(Eq.(25)).**	mM
$c_{\mathrm{B,tot}}^{\mathrm{W}}$	Total concentration of weak base in the aqueous phase **(Eq.(26)).**	mM
$c_{\mathrm{B}}^{\mathrm{a}}$	Analytical concentration of the weak base **(Eq.(25) and Eq.(26)).**	mM
$c_{\mathrm{B,tot}}^{\mathrm{init}}$	Total initial concentration of the weak base **(Eq.(27)).**	mM
$c_{\mathrm{SE}}^{\mathrm{O}}$	Concentration of the supporting electrolyte in the organic phase.	mM
$D_{\mathrm{species}}^{\mathrm{O}}$	Diffusion coefficient of species in the organic phase	$\mathrm{cm^2s^{-1}}$
$D_{\mathrm{species}}^{\mathrm{W}}$	Diffusion coefficient of species in the aqueous phase	$\mathrm{cm^2s^{-1}}$
D^{α}	Diffusion coefficient of HB^+, B or HBY in phase α.	$\mathrm{cm^2s^{-1}}$
$\bar{D}$	Effective diffusion coefficient for Red^- and KRed species.	$\mathrm{cm^2s^{-1}}$
E_{mid}	Mid-peak potential.	V
$K_{\mathrm{a,HB}^+}^{'\alpha}$	Apparent acid dissociation constant for species HB^+ in phase α **(Eq.(4)).**	Dimensionless
$K_{\mathrm{SE}}^{'}$	Apparent supporting electrolyte ion-pair equilibrium constant in the organic phase **(Eq.(5)).**	Dimensionless
$K_{\mathrm{KRed}}^{'}$	Apparent ion-pair equilibrium constant in the organic phase between Red^- species and the cation of the supporting electrolyte **(Eq.(6)).**	Dimensionless
$K_{\mathrm{HBY}}^{'}$	Apparent ion-pair equilibrium constant in the organic phase between species and the anion of the supporting electrolyte **(Eq.(7)).**	Dimensionless
$K_{\mathrm{D,B}}^{'}$	Apparent partition coefficient of the neutral species **(Eq.(8)).**	Dimensionless

$r = V_o V_w^{-1}$	Organic to aqueous phase volume ratio	Dimensionless
α_{SE}	Degree of dissociation of the supporting electrolyte	Dimensionless
α_B	Degree of dissociation of the weak base.	Dimensionless
$\gamma_{species}^{\alpha}$	Activity coefficient of species in phase α.	Dimensionless
$\Delta_O^S\phi_{1/2}$	Half-wave potential at the S|L interface.	V
$\Delta_O^W\phi_{1/2}$	Half-wave potential at the L|L interface.	V
$\Delta_O^S\phi^{o'}$	Formal standard reduction potential **(Eq.(20)).**	V
$\Delta_O^W\phi_{species}^{o'}$	Formal standard transfer potential of species across the L|L interface.	V
$\Delta_O^W\phi\left(\Delta_O^S\phi_{1/2}\right)$	Galvani potential difference at the L|L interface when the Galvani potential difference at the S|L interface is equal to $\Delta_O^S\phi_{1/2}$.	V
$\Delta_O^S\phi\left(\Delta_O^W\phi_{1/2}\right)$	Galvani potential difference at the S|L interface when the Galvani potential difference at the L|L interface is equal to $\Delta_O^W\phi_{1/2}$.	V
$\Delta\phi_{1/2}$	Half-wave potential of the FPT-ET reactions **(Eq.(36)).**	V

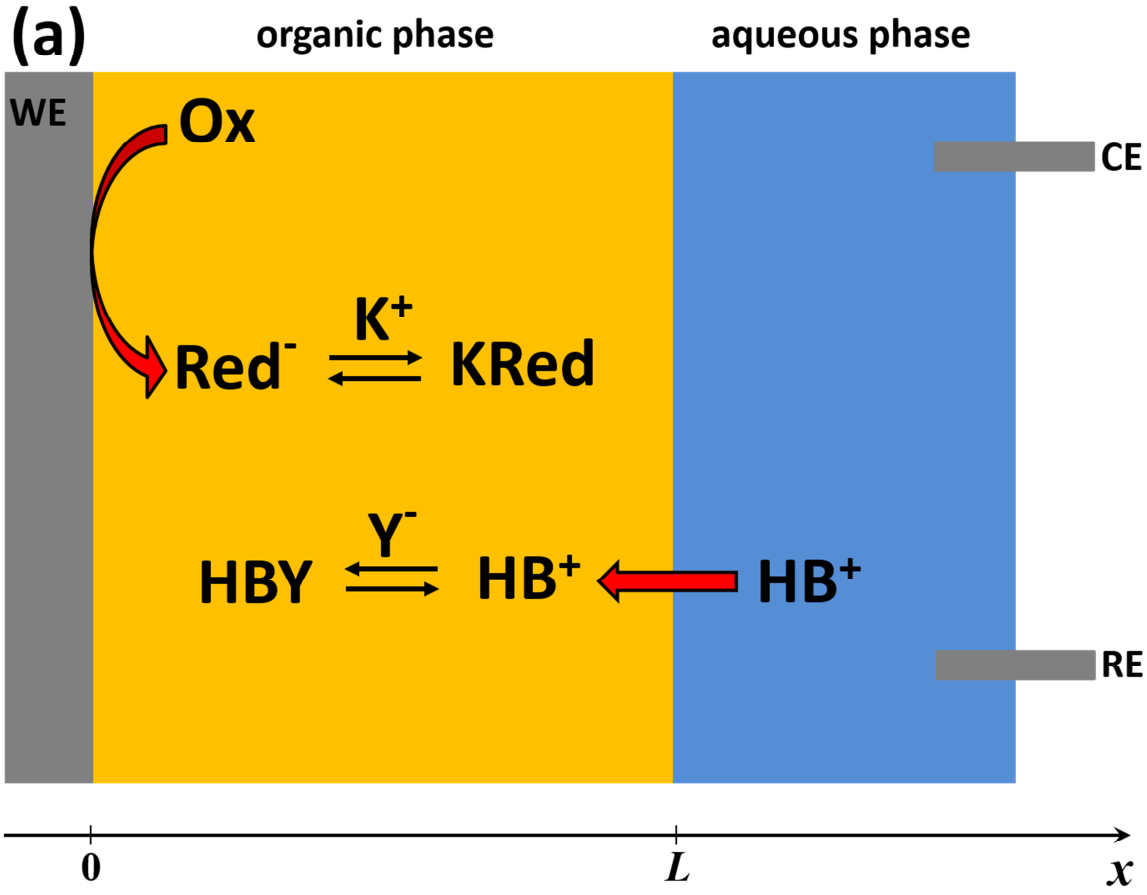
(a)
organic phase
aqueous phase
WE
Ox
CE
K+
Red-
KRed
Y-
HBY
HB+
HB+
RE
0
L
x

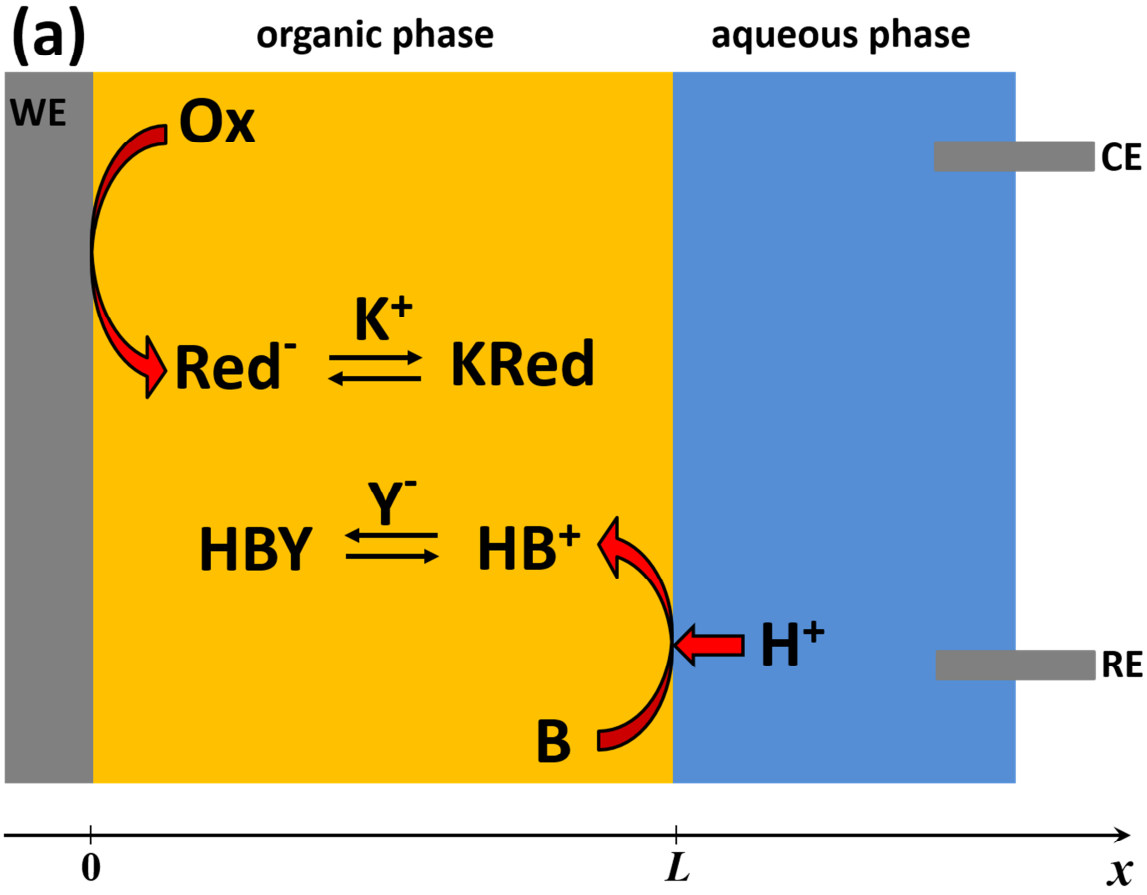
(a)
organic phase
aqueous phase
WE
Ox
CE
K+
Red-
KRed
Y-
HBY
HB+
H+
RE
B
0
L
x

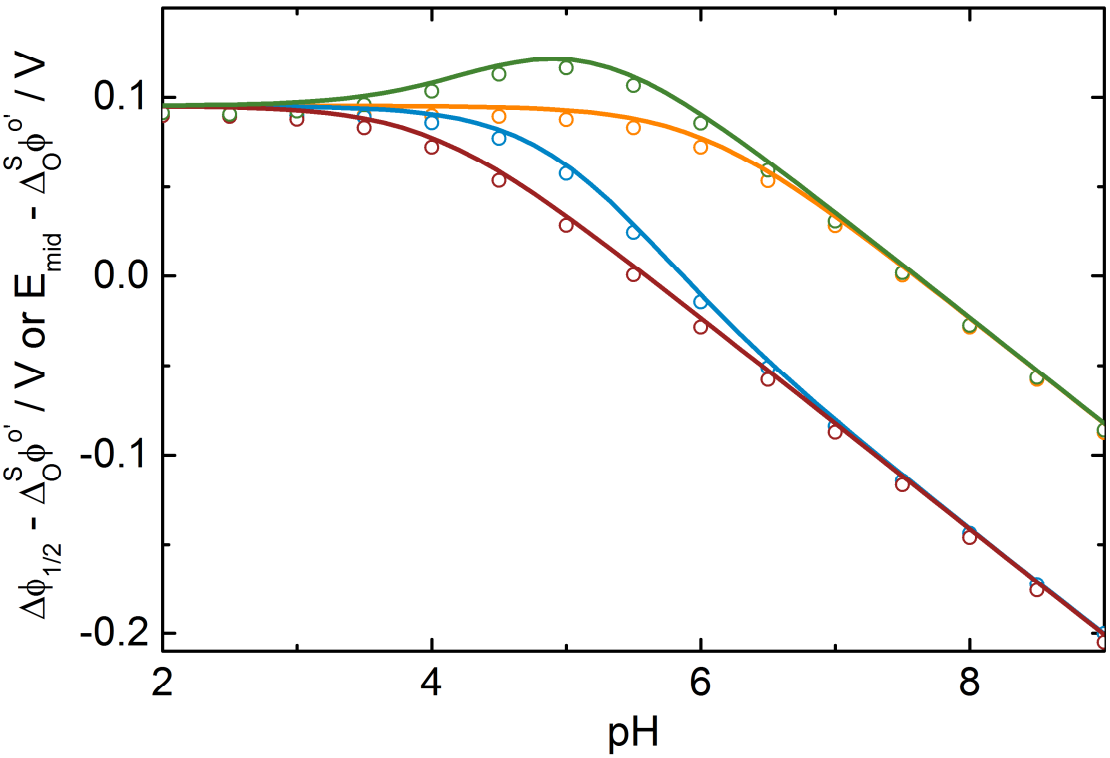

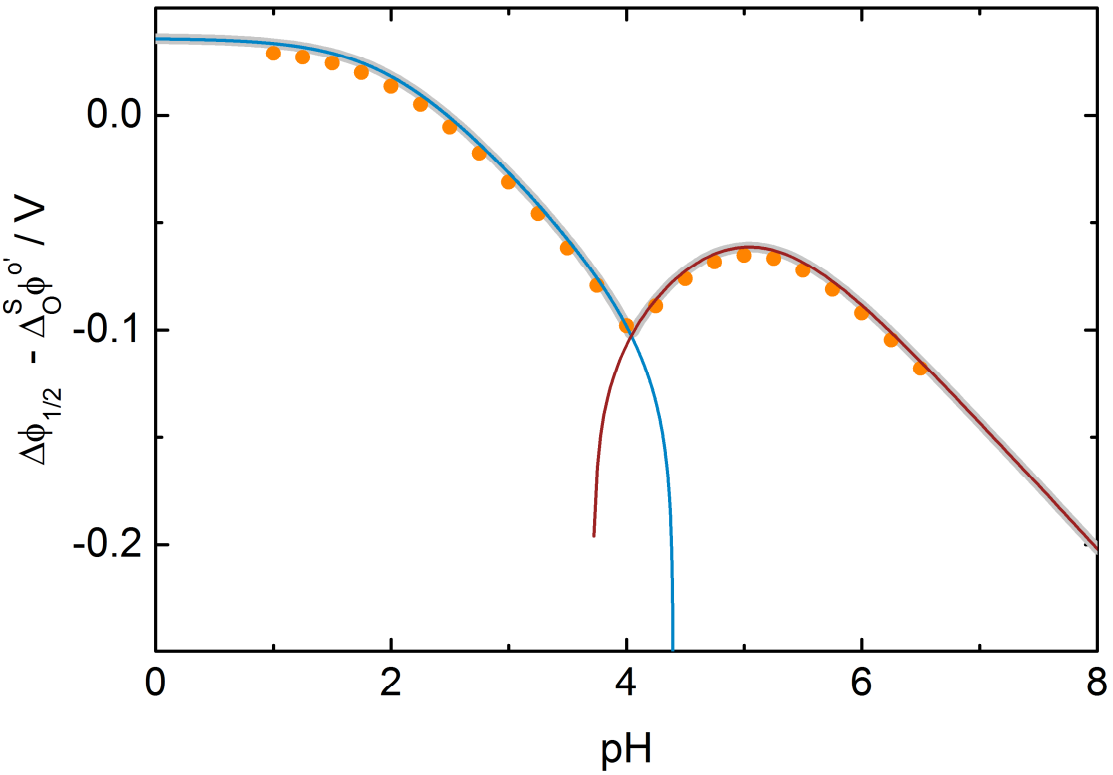

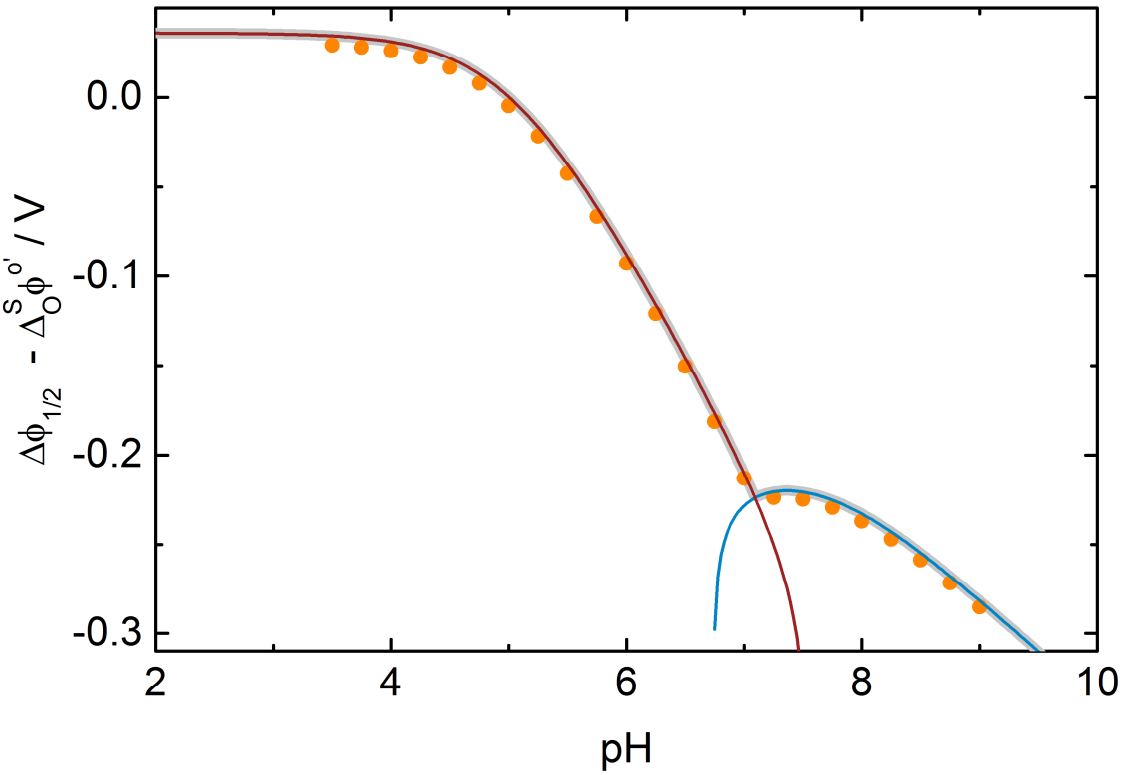

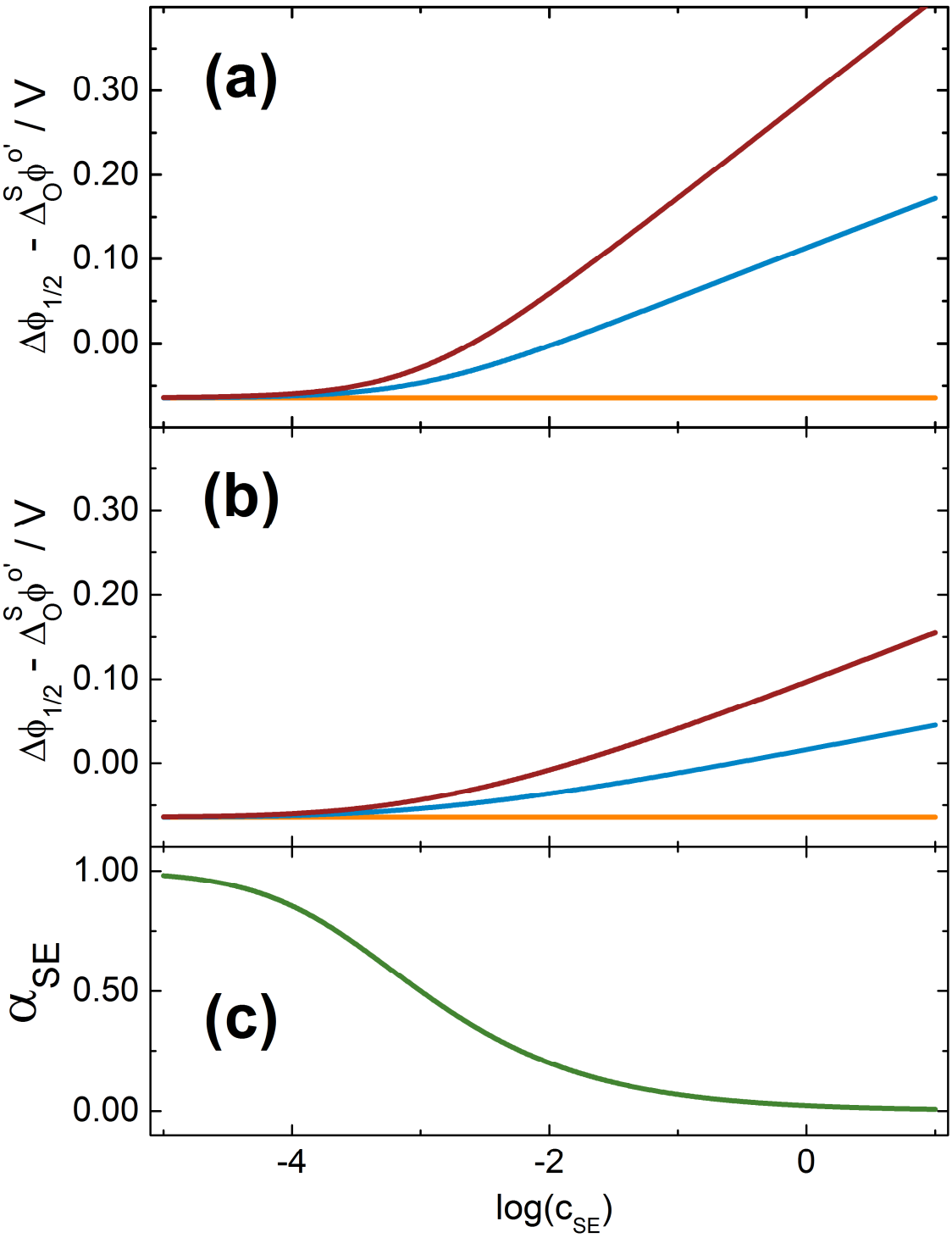
(a)
(b)
(c)
0.30
0.20
0.10
0.00
1.00
0.50
0.00
-4
-2
0
log(c_SE)
Δφ1/2 - ΔOφ°' / V
αSE

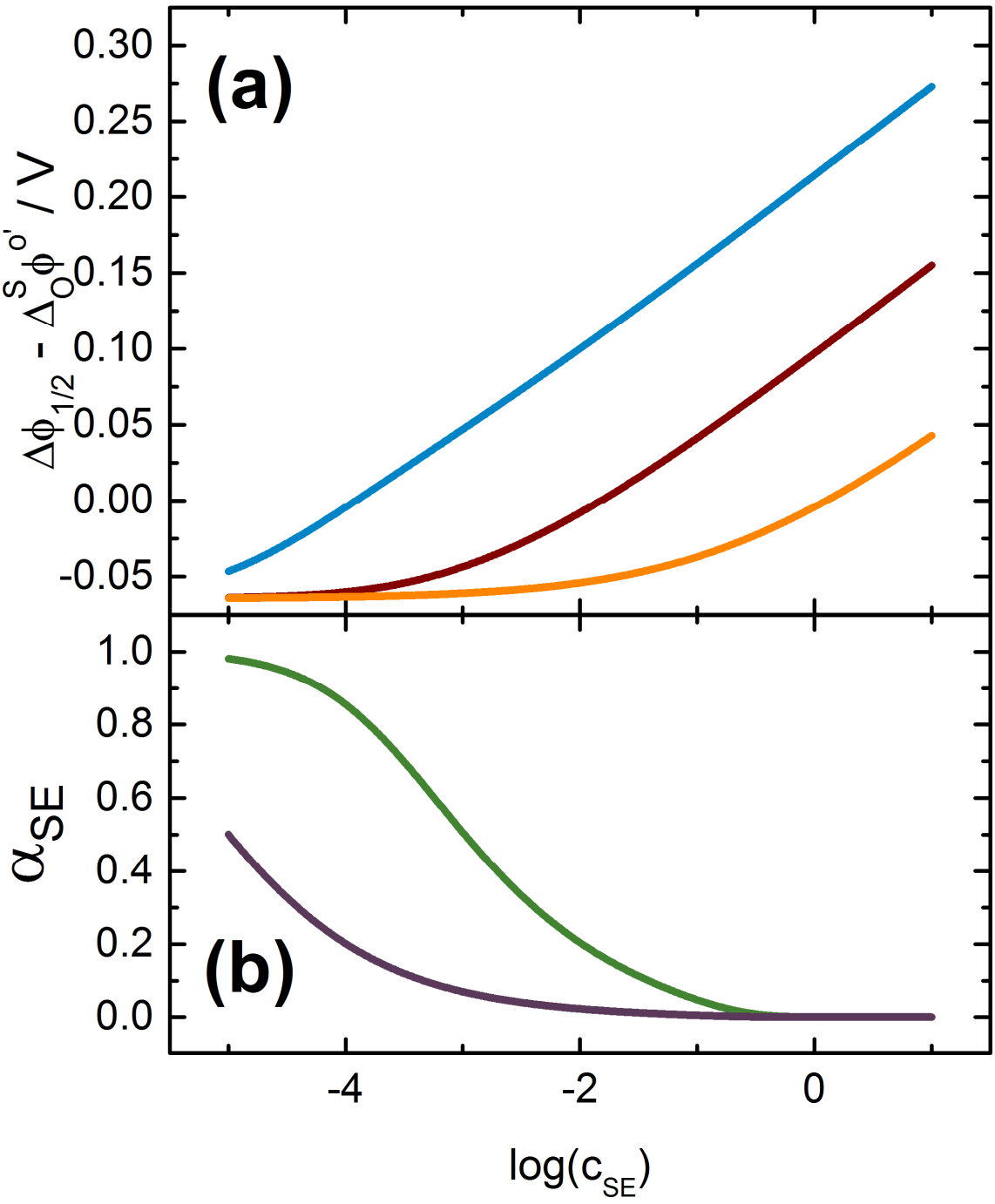
(a)
(b)
0.30
0.25
0.20
0.15
0.10
0.05
0.00
-0.05
$\Delta\phi_{1/2} - \Delta_O^S\phi^{o'}$ / V
1.0
0.8
0.6
0.4
0.2
0.0
α_{SE}
-4
-2
0
log(c_{SE})

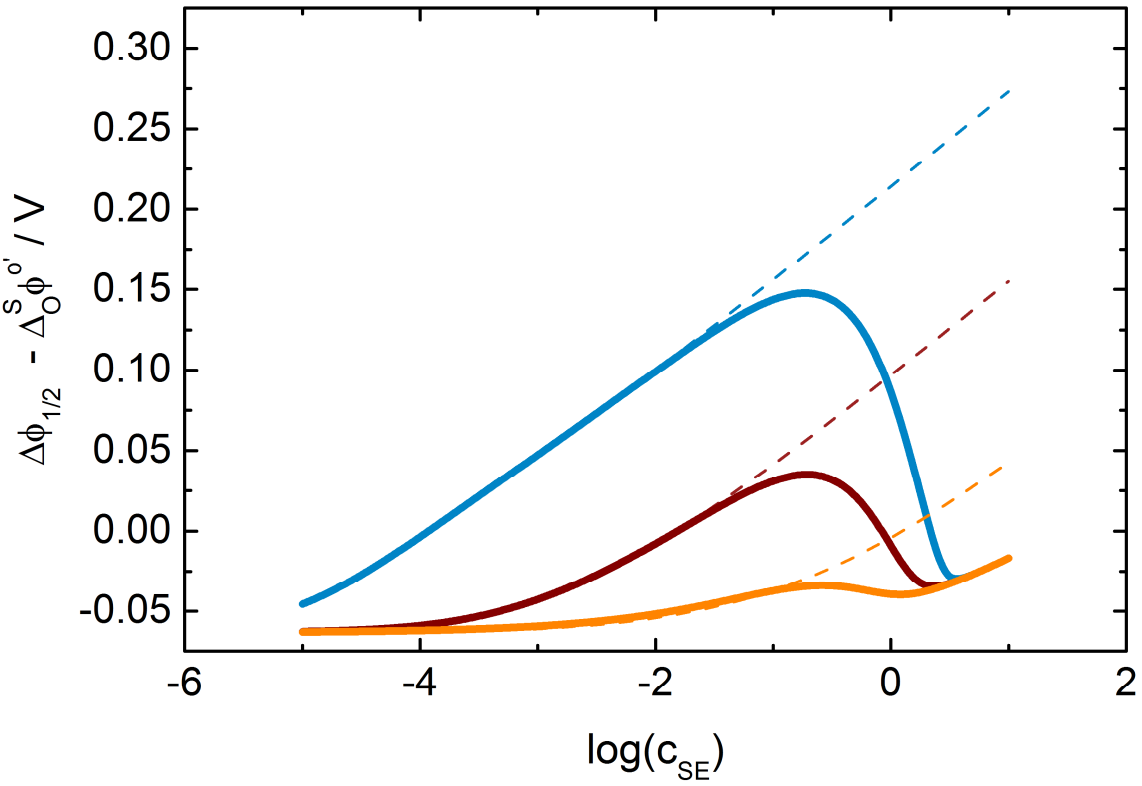

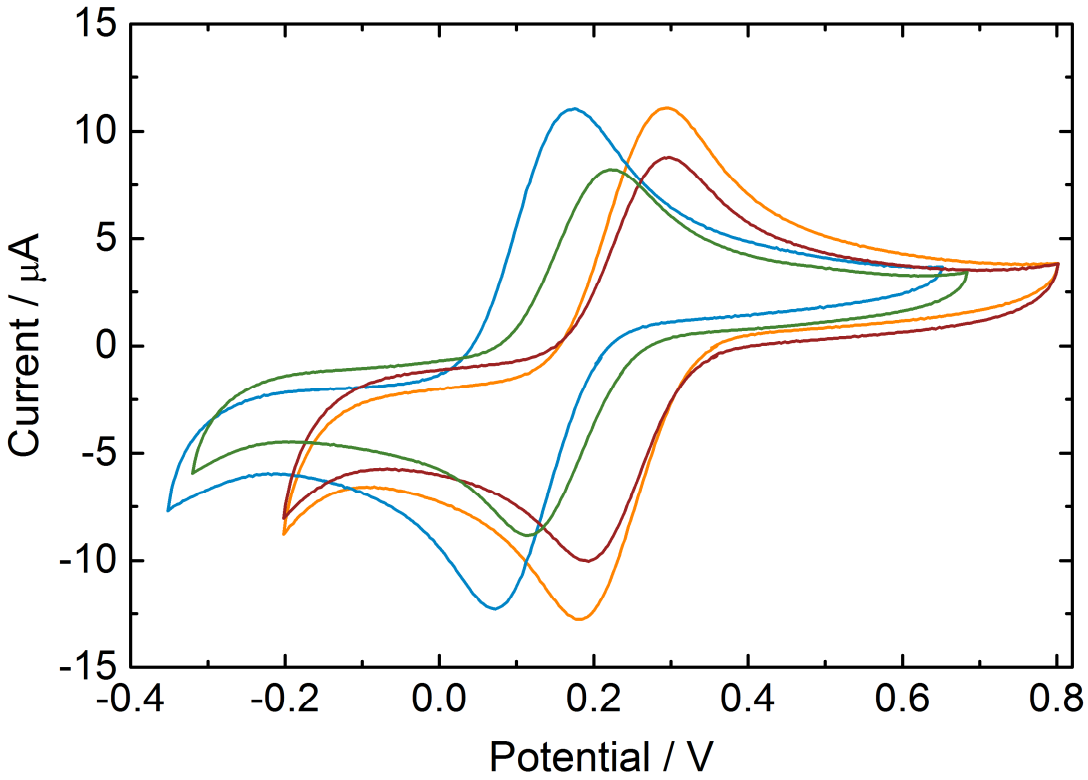

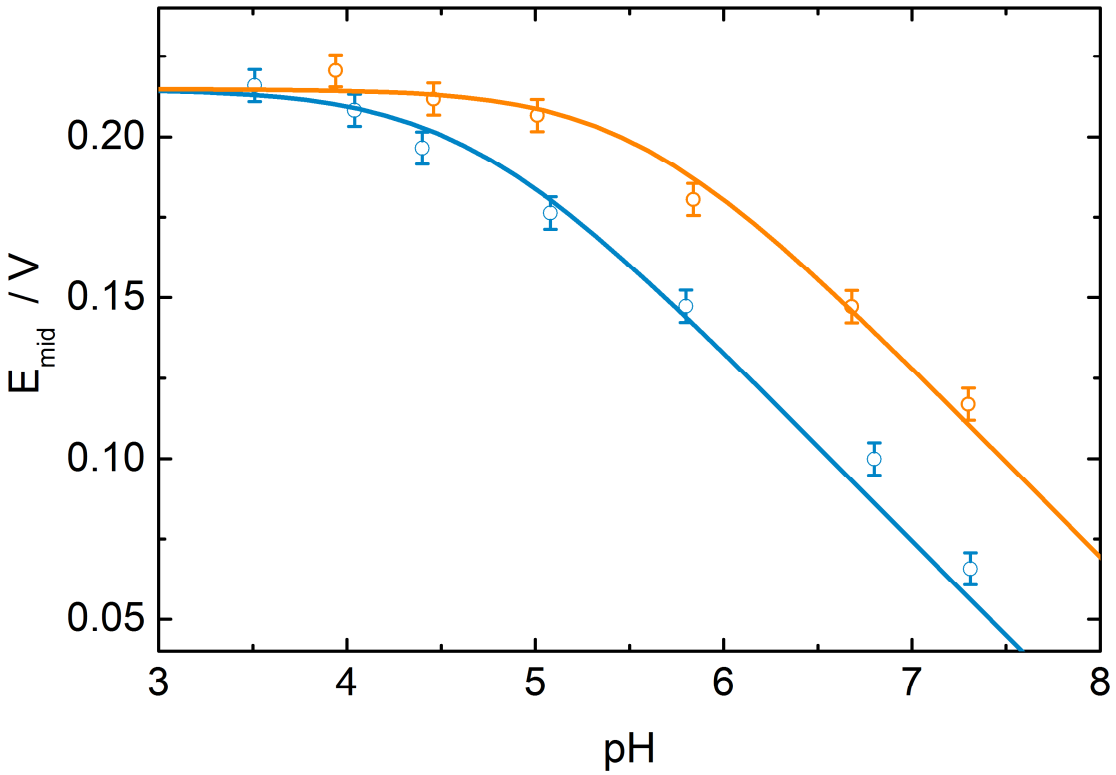

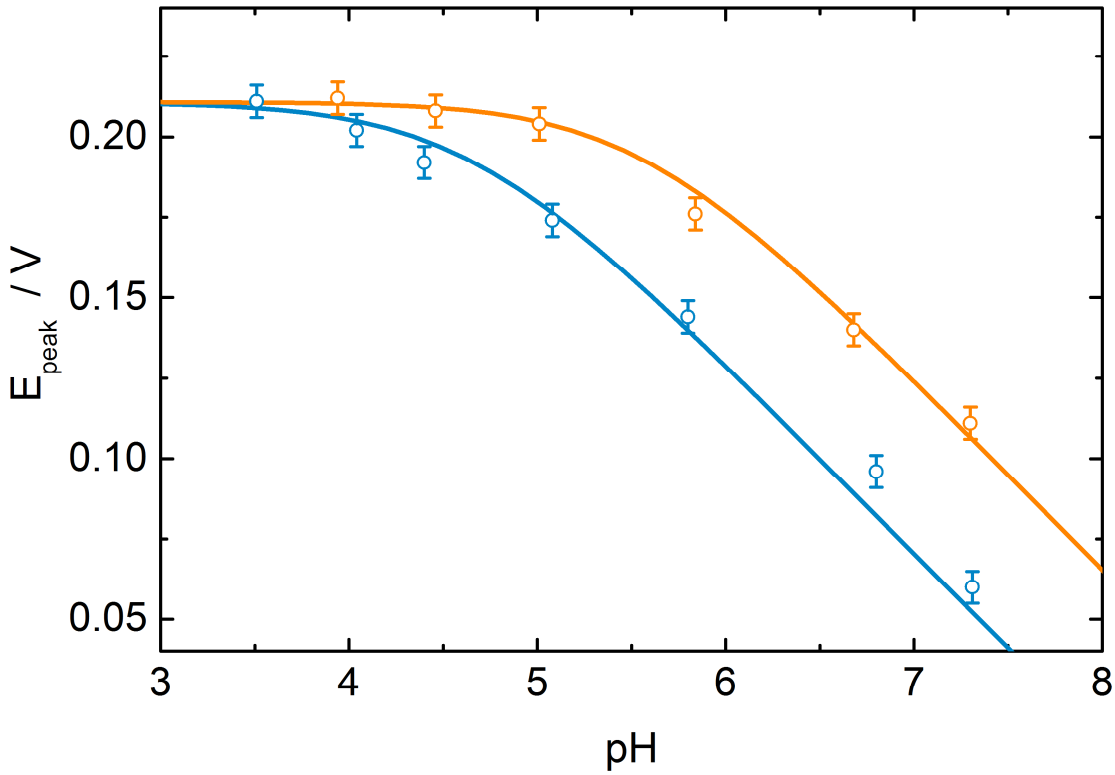

Highlights

> Weak base facilitated proton transfer is analysed for thick film modified electrodes.

> Analytical expressions for the half-wave potential are developed.

> Ion pairing and non-ideal electrolyte solutions are explicitly incorporated into the model.